

Interaction of an atom with layered dielectrics

Claudia Eberlein¹ and Robert Zietal¹

¹*Department of Physics & Astronomy, University of Sussex, Falmer, Brighton BN1 9QH, England*
(Dated: November 17, 2018)

We determine the energy-level shift experienced by a neutral atom due the quantum electromagnetic interaction with a layered dielectric body. We use the technique of normal-mode expansion to quantize the electromagnetic field in the presence of a layered, non-dispersive and non-absorptive dielectric. We explicitly calculate the equal-time commutation relations between the electric field and vector potential operators. We show that the commutator can be expressed in terms of a generalized transverse delta-function and that this is a consequence of using the generalized Coulomb gauge to quantize the electromagnetic field. These mathematical tools turn out to be very helpful in the calculation of the energy-level shift of the atom, which can be in its ground state or excited. The results for the shift are then analysed asymptotically in various regions of the system's parameter space – with a view to providing quick estimates of the influence of a single dielectric layer on the Casimir-Polder interaction between an atom and a dielectric half-space. We also investigate the impact of resonances between the wavelength of the atomic transition and the thickness of the top layer.

PACS numbers: 31.70.-f, 41.20.Cv, 42.50.Pq

I. INTRODUCTION

The question of the interaction between a neutral atom and a macroscopic dielectric body, once of purely academic interest, has recently been promoted to a real-life physics problem thanks to the rapid developments in nanotechnology and experimental techniques. It is no longer the case that this interaction, the so-called Casimir-Polder interaction, is a tiny effect that can be ignored in all practical situations. Instead, on the length-scales that nanotechnology nowadays operates in, dispersion forces, as they are also called, become significant and may appreciably influence miniaturized physical systems. Many of the current ambitions of cold-atom physics towards quantum computation and a variety of nanotechnological applications involves the trapping and accurate guiding of single atoms above dielectric substrates, so-called atom chips. With these the nearby environment of a trapped atom usually consists of a complicated array of inhomogeneous dielectrics. The questions then arising are: what are the magnitudes of the Casimir-Polder forces felt by the atom, and can one possibly engineer the types and shapes of surrounding materials either to minimize unwanted dispersion forces or to make them optimally contribute to the trapping or guiding? In order to investigate such possibilities one needs to go beyond simple featureless geometries and ground-state atoms and gain flexibility. The perhaps least sophisticated but still interesting example to study in this context is to consider a neutral atom, possibly excited, above a layered dielectric half-space, cf. Fig. 1. If the atom is in its ground state, then the Casimir-Polder force is always attractive for material surfaces with refractive indices greater than 1. In such case it is desirable to derive simple analytical formulae that would allow one to obtain quick estimates of the magnitudes of the forces involved in terms of the optical properties of the layer and the substrate

[1]. On the other hand, if the atom is in its excited state, then, as it is widely recognised [2], the potential acquires a oscillatory contribution that can result in a repulsive force. Additionally, the presence of the layer creates the possibility of a resonance between the wavelength of the atomic transition and the thickness of the layer, which could lead to a suppression or enhancement of the interaction.

There exist a variety of theoretical approaches devised to study the Casimir-Polder interaction (see e.g. [3] for a recent list of references) but perhaps the most successful ones being the linear response theory [4] and phenomenological macroscopic QED [5]. By using linear response theory [4] and expressing the field susceptibilities in terms of Fresnel reflection coefficients [2, 6], one can express the Casimir-Polder interaction as an integral along the imaginary frequency axis of the product of the atomic and field susceptibilities. Thus in practice the problem is reduced to the calculation of the classical electromagnetic Green's tensor expressed in terms of Fresnel coefficients. Such calculations, while straightforward in principle, tend to be quite tedious and often inevitably lead to the use of numerical methods. However, there is a benefit to studying problems in quantum electrodynamics by using physically transparent methods that do not obscure the basic underlying physics. For the kind of geometry of plane layered dielectrics considered in this paper, the technique of electromagnetic field quantization based on a normal-mode expansion [7] seems to be best emphasizing the physics of the problem, namely the fact that the system supports two kinds of modes of the electromagnetic field [8]: these are travelling modes with a continuous spectrum and trapped modes with a discrete spectrum, i.e. occurring at only certain allowed frequencies. The trapped modes arise because of repeated total internal reflections within the top layer of higher refractive index than the substrate, and emerge as evanescent

waves outside the wave-guide. This gives rise to an intricate assortment of evanescent modes outside a layered dielectric where evanescent waves with continuous spectrum, also arising in a half-space geometry [7], are superposed with discrete evanescent modes that arise only in the presence of the slab-like waveguide [1]. In the framework we apply in this work, in the same spirit as e.g. [1, 9], the use of standard perturbation theory renders all calculations explicit and it is possible from the outset to track down and remove if necessary any ambiguities that tend to remain hidden in more elaborate theories. For example, linear-response theory results in an integral over the Fresnel reflection coefficients but gives no indication of whether the evanescent waves associated with the trapped modes contribute to the Casimir-Polder interaction or not. The question is answered at once if the normal-modes approach is used instead, see [8, 11]. Also, interpretations of more complicated field-theoretical approaches [10] can be put to an explicit test [1].

The purpose of this paper is twofold. Firstly, it aims to support current experimental efforts by providing a range of analytical formulae useful for quick estimates of the dispersion forces acting on an atom placed in the vicinity of the layered dielectric, with particular emphasis on the corrections caused by the layer as compared to the standard half-space results reported in [9]. It also investigates the resonant interaction between an excited atom and a layer in the search for the possible enhancement or suppression of the Casimir-Polder force. Secondly, it formulates a simple and explicit theory based on well understood concepts of theoretical physics such as perturbation theory and electromagnetic field quantization in terms of a normal-modes expansion. The theoretical aspect, although serving only as a means to a practical end result, turns out to be interesting in its own right. The perturbative approach used in this work leads to the problem of the summation over the modes of the electromagnetic field, which is non-trivial because of the dual character of the modes of the electromagnetic field. The task of adding the discrete and continuous field modes is elegantly accomplished by the use of complex-integration techniques. This allows us to explicitly show that the canonical commutation relations between the field operators are satisfied, which is equivalent to saying that the completeness relation of the normal-modes holds in the geometry considered. Although this is not a surprise because the field modes are solutions of a Hermitean operator's eigenvalue problem, the explicit calculation we carry out provides us with the mathematics necessary to complete a typical perturbative calculation in this geometry. It also allows us to cast the end result in a simple and elegant form that is easy to study analytically in various asymptotic regimes. The same technique could be applied to any similar perturbative problem in such a geometry.

This paper is organised as follows. First we quantize the electromagnetic field in the presence of a layered dielectric, Section II. Then, in Section IIC, we explicitly

prove the completeness relation for the electromagnetic field modes. Equipped with the necessary mathematical tools, we proceed to calculate the energy shift in Section III, and then study it analytically (Section IV) and numerically (Section V).

II. FIELD QUANTIZATION IN THE PRESENCE OF A LAYERED BOUNDARY

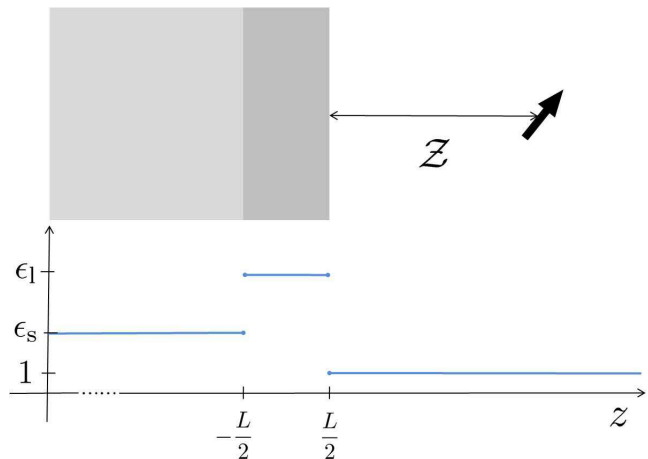


FIG. 1: Atomic dipole moment in the vicinity of the layered dielectric. The dielectric function is a piecewise constant function of the coordinate z .

Our ultimate aim is to work out the energy-level shift in an atom caused by the presence of a layered dielectric. In order to obtain a result that fully takes into account retardation effects, the quantization of the electromagnetic field is necessary. To emphasize the physics of the problem we choose to quantize the electromagnetic field by a normal-mode expansion as described in [12]. The dielectric environment we consider (cf. Fig. 1) consists of a substrate, a dielectric half-space occupying the region of space $z < -L/2$ described by a dielectric constant $\epsilon_s = n_s^2$, and on top of that substrate an additional dielectric layer of thickness L , which has a dielectric constant $\epsilon_1 = n_1^2$. We assume that the dielectric constant of the layer is higher than that of the substrate $\epsilon_1 > \epsilon_s$ in order to account for modes that are trapped inside the layer. Although we work with this assumption, the final result will turn out to be valid even when the reflectivity of the substrate exceeds that of the layer, but that is the physically less interesting case. Throughout this paper we shall assume all dielectric constants to be frequency independent so that the optical properties of the system are described solely by a pair of real numbers, ϵ_1 and ϵ_s .

To solve Maxwell equations for the electromagnetic field operators in the Heisenberg's picture we introduce, in the usual manner [13], the electromagnetic potentials $\mathbf{A}(\mathbf{r}, t)$ and $\Phi(\mathbf{r}, t)$ and work in the generalized Coulomb

gauge

$$\nabla \cdot [\epsilon(\mathbf{r})\mathbf{A}(\mathbf{r})] = 0, \quad (1)$$

with the dielectric permittivity being a piecewise constant function as shown in Fig. 1. In the absence of free charges one can set $\Phi(\mathbf{r}, t) = 0$ and work only with the vector potential $\mathbf{A}(\mathbf{r}, t)$ which satisfies the wave equation

$$\nabla^2 \mathbf{A}(\mathbf{r}, t) - \epsilon(z) \frac{\partial^2}{\partial t^2} \mathbf{A}(\mathbf{r}, t) = 0, \quad |z| \neq L/2. \quad (2)$$

Note that right on the interfaces condition (1) is singular due to discontinuities of the dielectric function and equation (2) does not hold at these points. The normal-modes of the field $\mathbf{f}(\mathbf{r})e^{i\omega t}$ satisfy the Helmholtz equation

$$\nabla^2 \mathbf{f}_{\mathbf{k}\lambda}(\mathbf{r}) + \epsilon(z)\omega^2 \mathbf{f}_{\mathbf{k}\lambda}(\mathbf{r}) = 0, \quad |z| \neq L/2, \quad (3)$$

and we have labelled them by their wave-vector \mathbf{k} and polarization $\lambda = \{\text{TE}, \text{TM}\}$. This mode decomposition allows one to solve the field equation (2) in each distinct region of space separately and then stitch up the solutions across the interfaces by demanding that they are consistent with the Maxwell boundary conditions, i.e. that \mathbf{E}_{\parallel} , D_{\perp} , and \mathbf{B} are all continuous.

The Helmholtz equation (3) is in fact the eigenvalue problem of an Hermitean operator[12]

$$\left[\frac{1}{\sqrt{\epsilon}} \nabla \times \nabla \times \frac{1}{\sqrt{\epsilon}} \right] \sqrt{\epsilon} \mathbf{f}_{\mathbf{k}\lambda}(\mathbf{r}) = -\omega^2 \sqrt{\epsilon} \mathbf{f}_{\mathbf{k}\lambda}(\mathbf{r}), \quad (4)$$

so that we expect the field modes $\sqrt{\epsilon} \mathbf{f}_{\mathbf{k}\lambda}(\mathbf{r})$ to form a complete set of functions suitable for describing any field configuration. The completeness relation takes the form

$$\int d^2 \mathbf{k}_{\parallel} \sum_{k_z} f_{\mathbf{k}\lambda}^i(\mathbf{r}) f_{\mathbf{k}\lambda}^{*j}(\mathbf{r}') = \delta_{ij}^{\epsilon}(\mathbf{r}, \mathbf{r}'), \quad z, z' > L/2 \quad (5)$$

with $\delta_{ij}^{\epsilon}(\mathbf{r}, \mathbf{r}')$ being the unit kernel in the subspace of functions satisfying (1); we shall call this the generalized transverse delta-function. From quite general considerations [14] we can expect it to be given by

$$\delta_{ij}^{\epsilon}(\mathbf{r}, \mathbf{r}') = \delta_{ij} \delta^{(3)}(\mathbf{r} - \mathbf{r}') - \nabla_i \nabla_j' G(\mathbf{r}, \mathbf{r}') \quad (6)$$

with the electrostatic Green's function of the Laplace equation given by

$$G(\mathbf{r}, \mathbf{r}') = \frac{1}{4\pi} \frac{1}{|\mathbf{r} - \mathbf{r}'|} - \frac{1}{4\pi} \int_0^{\infty} dk J_0(k\rho) e^{-k(z+z')} \\ \times \frac{\frac{n_1^2 - 1}{n_1^2 + 1} - \frac{n_1^2 - n_s^2}{n_s^2 + n_1^2} e^{-2kL}}{1 - \frac{n_1^2 - 1}{n_1^2 + 1} \frac{n_1^2 - n_s^2}{n_s^2 + n_1^2} e^{-2kL}} \quad (7)$$

where $\rho = |\mathbf{r}_{\parallel} - \mathbf{r}'_{\parallel}|$ and, for brevity, we have chosen to confine ourselves to the case $z, z' > L/2$. The function J_0 in the above equation is a Bessel function of the first kind

[15, 9.1.1]. The outline of the derivation of the Green's function is given in Appendix B.

The sum over all modes in equation (5) is complicated because the spectrum of the field modes has non-trivial structure. It has been shown previously [8, 16] that the system supports two kinds of quite distinct types of modes. There are travelling modes going from left to right or in the opposite direction, and there are guided modes that are trapped by the dielectric layer, which essentially acts as a wave-guide. The spectrum of the travelling modes is continuous whereas the spectrum of the modes trapped in the dielectric layer is discrete and only some values of the (perpendicular) wave vector are allowed, namely those satisfying a certain dispersion relation. This dual character of the spectrum of the field modes is a major obstacle in working with these modes and calculating, e.g. the energy shift of an atom nearby, but an elegant solution to this problem has been developed in [17], whose basic idea we follow here.

We choose the normalization of the mode functions $\sqrt{\epsilon} \mathbf{f}_{\mathbf{k}\lambda}(\mathbf{r})$ according to the convention

$$\int d^3 \mathbf{r} \epsilon(z) \mathbf{f}_{\mathbf{k}\lambda}^*(\mathbf{r}) \cdot \mathbf{f}_{\mathbf{k}'\lambda'}(\mathbf{r}) = \begin{cases} \delta_{\lambda\lambda'} \delta^{(3)}(\mathbf{k} - \mathbf{k}') & \text{travelling modes} \\ \delta_{\lambda\lambda'} \delta^{(2)}(\mathbf{k}_{\parallel} - \mathbf{k}'_{\parallel}) \delta_{k_z k'_z} & \text{trapped modes} \end{cases} \quad (8)$$

Then, the electric field $\mathbf{E}(\mathbf{r}) = -\partial_t \mathbf{A}(\mathbf{r})$ expanded in terms of the normal-modes can be written as

$$\mathbf{E}(\mathbf{r}) = i \sum_{\lambda} \int d^2 \mathbf{k}_{\parallel} \sum_{k_z} \sqrt{\frac{\omega_{\mathbf{k}}}{2\epsilon_0}} a_{\mathbf{k}\lambda} \mathbf{f}_{\mathbf{k}\lambda}(\mathbf{r}) e^{-i\omega_{\mathbf{k}} t} + \text{H.C.} \quad (9)$$

where H.C. stands for Hermitean conjugate. The photon creation and annihilation operators, $a_{\mathbf{k}\lambda}^{\dagger}$ and $a_{\mathbf{k}\lambda}$, satisfy bosonic commutation relation

$$[a_{\mathbf{k}\lambda}, a_{\mathbf{k}\lambda'}^{\dagger}] = \delta_{\lambda\lambda'} \begin{cases} \delta^{(3)}(\mathbf{k} - \mathbf{k}') \\ \delta^{(2)}(\mathbf{k}_{\parallel} - \mathbf{k}'_{\parallel}) \delta_{k_z k'_z} \end{cases}, \quad (10)$$

where the top and bottom of the RHS corresponds to the travelling and trapped photons, respectively. In order to be able to write out the electromagnetic field operators explicitly one needs to solve the eigenvalue problem (3) and determine the spatial dependence of functions $\mathbf{f}_{\mathbf{k}\lambda}(\mathbf{r})$ so we turn our attention to this now.

A. Travelling modes

Before we work out the travelling modes, for further convenience, we introduce Fresnel coefficients for a single interface. For that we assume that a plane wave is travelling from a medium with refractive index n_b to a medium with the refractive index n_a , and that the interface is the $z = 0$ plane. Then, the standard Fresnel reflection and

transmission coefficients are given by [13]

$$\begin{aligned} r_{\text{TE}}^{\text{ba}} &= \frac{k_{\text{zb}} - k_{\text{za}}}{k_{\text{zb}} + k_{\text{za}}}, & t_{\text{TE}}^{\text{ba}} &= \frac{2k_{\text{zb}}}{k_{\text{zb}} + k_{\text{za}}}, \\ r_{\text{TM}}^{\text{ba}} &= \frac{k_{\text{zb}}/n_{\text{b}}^2 - k_{\text{za}}/n_{\text{a}}^2}{k_{\text{zb}}/n_{\text{b}}^2 + k_{\text{za}}/n_{\text{a}}^2}, & t_{\text{TM}}^{\text{ba}} &= \frac{2k_{\text{zb}}/n_{\text{a}}n_{\text{b}}}{k_{\text{zb}}/n_{\text{b}}^2 + k_{\text{za}}/n_{\text{a}}^2}, \end{aligned} \quad (11)$$

where k_{zi} are the components of the wave vectors perpendicular to the interface in the medium $i = \{\text{a}, \text{b}\}$.

The geometry of the problem (cf. Fig. 1) naturally divides the space into three distinct regions. Consequently there are three wave vectors to be distinguished. The wave vector in vacuum ($z > L/2$)

$$\mathbf{k}^{\pm} = (k_x, k_y, \pm k_z) = (\mathbf{k}_{\parallel}, \pm k_z), \quad (12)$$

the wave vector in the dielectric layer ($|z| < L/2$)

$$\mathbf{k}_1^{\pm} = (k_x, k_y, \pm k_{z1}) = (\mathbf{k}_{\parallel}, \pm k_{z1}), \quad (13)$$

and the wavevector in the substrate ($z < -L/2$)

$$\mathbf{k}_s^{\pm} = (k_x, k_y, \pm k_{zs}) = (\mathbf{k}_{\parallel}, \pm k_{zs}). \quad (14)$$

The components of the wave vector that are parallel to the surface are the same for all three regions of space. This follows directly from the requirement that the boundary conditions must be satisfied at all points of a given surface i.e. the spatial phase factors $e^{i\mathbf{k}_i \cdot \mathbf{r}}$ must be equal at $z = \pm L/2$ for all \mathbf{r}_{\parallel} . The different signs of the z -components of the wave vectors correspond to the waves propagating in different directions. However, the direction of the propagation of a particular mode needs to be consistent in all three layers so we require that on the real axis

$$\text{sign}(k_z) = \text{sign}(k_{z1}) = \text{sign}(k_{zs}). \quad (15)$$

Since the frequency ω of a single mode is fixed, the z -components of the wave vectors in the dielectric are related to the vacuum wave vector k_z by

$$k_{z1} = \sqrt{(n_1^2 - 1)\mathbf{k}_{\parallel}^2 + n_1^2 k_z^2}, \quad (16)$$

$$k_{zs} = \sqrt{(n_s^2 - 1)\mathbf{k}_{\parallel}^2 + n_s^2 k_z^2}. \quad (17)$$

The mode functions $\mathbf{f}_{\mathbf{k}\lambda}(\mathbf{r})$ are transverse everywhere except right on the interfaces $z = \pm L/2$, cf. (1). To ensure this transversality, it is convenient to introduce orthonormal polarisation vectors

$$\mathbf{f}_{\mathbf{k}\lambda}(\mathbf{r}) = \hat{\mathbf{e}}_{\lambda}(\mathbf{k}) f_{\mathbf{k}\lambda}(\mathbf{r}) \quad (18)$$

defined as

$$\begin{aligned} \hat{\mathbf{e}}_{\text{TE}}(\nabla) &= (-\Delta_{\parallel})^{-1/2} (-i\nabla_y, i\nabla_x, 0), \\ \hat{\mathbf{e}}_{\text{TM}}(\nabla) &= (\Delta_{\parallel} \Delta)^{-1/2} (-\nabla_x \nabla_z, -\nabla_y \nabla_z, \Delta_{\parallel}), \end{aligned} \quad (19)$$

with Δ being the Laplace operator expressed in Cartesian coordinates and it is understood that the above

operators act on the factors of the type $e^{i\mathbf{k}_i^{\pm} \cdot \mathbf{r}}$, i.e. $\hat{\mathbf{e}}_{\lambda}(\mathbf{k}_i^{\pm}) \equiv \hat{\mathbf{e}}_{\lambda}(\nabla) e^{i\mathbf{k}_i^{\pm} \cdot \mathbf{r}}$. Polarization vectors defined in such a way are normalized to unity provided all three components of the wave vector are real. However, they are not of unit length in the case of evanescent waves which have wave vectors with pure imaginary components. The spatial dependence of the mode functions is worked out requiring that each mode consists of the incoming, reflected and transmitted parts that are joined together by standard boundary conditions across the interfaces, i.e. that \mathbf{E}_{\parallel} , D_{\perp} and \mathbf{B} are continuous. From this it is straightforward to derive that the travelling modes of the system incident from the left, normalized according to (8), are given by

$$\mathbf{f}_{\mathbf{k}\lambda}^L(\mathbf{r}) = \frac{\hat{\mathbf{e}}_{\lambda}(\nabla)}{(2\pi)^{\frac{3}{2}} n_s} \begin{cases} e^{i\mathbf{k}_s^+ \cdot \mathbf{r}} + R_{\lambda}^L e^{i\mathbf{k}_s^- \cdot \mathbf{r}} & z < -L/2 \\ I_{\lambda}^L e^{i\mathbf{k}_1^+ \cdot \mathbf{r}} + J_{\lambda}^L e^{i\mathbf{k}_1^- \cdot \mathbf{r}} & |z| < L/2 \\ T_{\lambda}^L e^{i\mathbf{k}^+ \cdot \mathbf{r}} & z > L/2 \end{cases}, \quad (20)$$

whereas the right-incident modes are given by

$$\mathbf{f}_{\mathbf{k}\lambda}^R(\mathbf{r}) = \frac{\hat{\mathbf{e}}_{\lambda}(\nabla)}{(2\pi)^{\frac{3}{2}}} \begin{cases} T_{\lambda}^R e^{i\mathbf{k}_s^- \cdot \mathbf{r}} & z < -L/2 \\ I_{\lambda}^R e^{i\mathbf{k}_1^- \cdot \mathbf{r}} + J_{\lambda}^R e^{i\mathbf{k}_1^+ \cdot \mathbf{r}} & |z| < L/2 \\ e^{i\mathbf{k}^- \cdot \mathbf{r}} + R_{\lambda}^R e^{i\mathbf{k}^+ \cdot \mathbf{r}} & z > L/2 \end{cases}. \quad (21)$$

For the sake of clarity the complete list of reflection and transmission coefficients is given in Appendix A. Here we only write down the ones most relevant for the calculation at hand:

$$R_{\lambda}^R = \frac{r_{\lambda}^{\text{vl}} + r_{\lambda}^{\text{ls}} e^{2ik_{z1}L}}{1 + r_{\lambda}^{\text{vl}} r_{\lambda}^{\text{ls}} e^{2ik_{z1}L}} e^{-ik_z L}, \quad (22)$$

$$T_{\lambda}^L = \frac{t_{\lambda}^{\text{sl}} t_{\lambda}^{\text{lv}} e^{(2ik_{z1} - ik_{zs} - ik_z)L/2}}{1 + r_{\lambda}^{\text{sl}} r_{\lambda}^{\text{lv}} e^{2ik_{z1}L}}. \quad (23)$$

B. Trapped modes

Trapped modes arise from repeated total internal reflections within the layer of higher refractive index n_1 . This happens when the angle of incidence of the incoming wave is sufficiently high and exceeds the critical angle. This critical angle is different for the two opposite waveguide interfaces. First consider the layer-vacuum interface. From equation (16) we can obtain the reciprocal relation expressing the k_z in terms of the k_{z1}

$$k_z = \frac{1}{n_1} \sqrt{k_{z1}^2 - (n_1^2 - 1)\mathbf{k}_{\parallel}^2}. \quad (24)$$

Thus, whenever $k_{z1}^2 < (n_1^2 - 1)\mathbf{k}_{\parallel}^2$ then k_z becomes pure imaginary

$$k_z = +\frac{i}{n_1} \sqrt{(n_1^2 - 1)\mathbf{k}_{\parallel}^2 - k_{z1}^2}, \quad (25)$$

and we have a mode that exhibits evanescent behaviour on the vacuum side. The sign of the square root is chosen such that these modes decay exponentially when one goes away from the layer in the positive z -direction. This also ensures that there truly is total internal reflection, i.e. that $|r_\lambda^{\text{vl}}|^2 = 1$.

However, since on the other side of the waveguide we have a substrate rather than vacuum, not all of the modes that get totally internally reflected at the vacuum-layer interface necessarily get trapped. From the relation

$$k_{zs} = \frac{n_s}{n_1} \sqrt{k_{z1}^2 - \mathbf{k}_\parallel^2 \left(\frac{n_1^2}{n_s^2} - 1 \right)} \quad (26)$$

we obtain the condition of total internal reflection for the substrate-layer interface to be $k_{z1}^2 \leq (n_1^2/n_s^2 - 1)\mathbf{k}_\parallel^2$. Therefore, modes satisfying the condition

$$(n_1^2/n_s^2 - 1)\mathbf{k}_\parallel^2 \leq k_{z1}^2 \leq (n_1^2 - 1)\mathbf{k}_\parallel^2 \quad (27)$$

are not trapped but appear in vacuum as a continuous spectrum of evanescent waves that are accounted for among the left-incident travelling modes. (They are analogous to the evanescent modes that occur at a single-interface half-space, for which the normal-mode quantization was first presented in [7].) On the other hand, trapped modes occur if

$$0 \leq k_{z1}^2 \leq (n_1^2/n_s^2 - 1)\mathbf{k}_\parallel^2. \quad (28)$$

The procedure for obtaining the trapped modes is largely equivalent to that of the travelling modes. They can be written in the form

$$\mathbf{f}_{\mathbf{k}\lambda}^T(\mathbf{r}) = N_\lambda \hat{\mathbf{e}}_\lambda(\nabla) \begin{cases} T_\lambda^{\text{ls}} e^{i\mathbf{k}_s^- \cdot \mathbf{r}} & z < -L/2 \\ V_\lambda e^{i\mathbf{k}_1^- \cdot \mathbf{r}} + e^{i\mathbf{k}_1^+ \cdot \mathbf{r}} & |z| < L/2 \\ T_\lambda^{\text{lv}} e^{i\mathbf{k}^+ \cdot \mathbf{r}} & z > L/2 \end{cases}. \quad (29)$$

The boundary conditions are imposed on both interfaces. From the boundary at $z = -L/2$ we get

$$\begin{aligned} T_\lambda^{\text{ls}} &= (t_\lambda^{\text{ls}}/r_\lambda^{\text{ls}}) e^{-i(k_{z1} + k_{zs})L/2}, \\ V_\lambda &= (1/r_\lambda^{\text{ls}}) e^{-ik_{z1}L}, \end{aligned} \quad (30)$$

whereas from the $z = L/2$ boundary

$$\begin{aligned} T_\lambda^{\text{lv}} &= t_\lambda^{\text{lv}} e^{-i(k_{z1} - k_z)L/2}, \\ V_\lambda &= r_\lambda^{\text{lv}} e^{ik_{z1}L}. \end{aligned} \quad (31)$$

Since both equations, (30) and (31), need to be simultaneously satisfied we obtain a dispersion relation for these modes,

$$1 + r_\lambda^{\text{vl}} r_\lambda^{\text{ls}} e^{2ik_{z1}L} = 0, \quad (32)$$

which determines the allowed values of k_{z1} within the layer. Since we will be dealing with an atom on the vacuum side it will be necessary to express the dispersion

relation in terms of k_z rather than k_{z1} . It is straightforward to show that the allowed values of the z -component of the evanescent waves' wave vector appearing on the vacuum side are given by numbers q_λ^n :

$$\begin{aligned} q_{\text{TE}}^n &= \{k_z : k_z + ik_{z1}(k_z) \tan[\phi_{\text{TE}}(k_z)] = 0\}, \\ q_{\text{TM}}^n &= \{k_z : k_z + ik_{z1}(k_z)/n_1^2 \tan[\phi_{\text{TM}}(k_z)] = 0\}, \end{aligned} \quad (33)$$

with

$$\begin{aligned} \phi_{\text{TE}}(k_z) &= \arg[(k_{z1} + k_{zs})e^{-ik_{z1}L}], \\ \phi_{\text{TM}}(k_z) &= \arg[(k_{z1}/n_1^2 + k_{zs}/n_s^2)e^{-ik_{z1}L}]. \end{aligned}$$

The numbers q_λ^n lie on the imaginary k_z -axis; they satisfy, cf. Eq. (25) and (28),

$$\left(\frac{1}{n_1^2} - 1 \right) \mathbf{k}_\parallel^2 < (q_\lambda^n)^2 < \left(\frac{1}{n_s^2} - 1 \right) \mathbf{k}_\parallel^2. \quad (34)$$

The normalization constant N_λ for trapped modes is easily obtained by direct evaluation of the integral (8). It is given by

$$N_\lambda = \frac{1}{2\pi} \left[2n_1^2 L + F_\lambda(n_1, n_s) + F_\lambda(n_1, 1) \right]^{-1/2} \quad (35)$$

with

$$\begin{aligned} F_\lambda(n_1, n_s) &= \frac{n_s^2}{2} |\hat{\mathbf{e}}_\lambda(\mathbf{k}_s^-)|^2 \frac{|t_\lambda^{\text{ls}}|^2}{|k_{zs}|} \\ &\quad - \frac{n_1}{k_{z1}} \text{Im}(r_\lambda^{\text{ls}}) \hat{\mathbf{e}}_\lambda^*(\mathbf{k}_1^+) \cdot \hat{\mathbf{e}}_\lambda(\mathbf{k}_1^-) \end{aligned}$$

and the reader is reminded that in (35) the z -components of the wave vectors \mathbf{k} and \mathbf{k}_s are pure imaginary and because of that the TM polarization vectors $\hat{\mathbf{e}}_{\text{TM}}(\mathbf{k}^-)$ and $\hat{\mathbf{e}}_{\text{TM}}(\mathbf{k}_s^-)$ are no longer normalized to unity, i.e. $|\hat{\mathbf{e}}_{\text{TM}}(\mathbf{k}_s^-)|^2 \neq 1$.

C. Field operators and commutation relations. Completeness of the modes.

Now that we have determined the spatial dependence of the mode functions we are in position to write out the vector potential field operator explicitly

$$\begin{aligned} \hat{\mathbf{A}}(\mathbf{r}, t) &= \left\{ \int d^2\mathbf{k}_\parallel \int_0^\infty dk_z \frac{1}{\sqrt{2\epsilon_0\omega_{\mathbf{k}}}} \mathbf{f}_{\mathbf{k}\lambda}^R(\mathbf{r}) a_{\mathbf{k}\lambda}^R e^{-i\omega_{\mathbf{k}}t} \right. \\ &\quad + \int d^2\mathbf{k}_\parallel \int_0^\infty dk_{zs} \frac{1}{\sqrt{2\epsilon_0\omega_{\mathbf{k}}}} \mathbf{f}_{\mathbf{k}\lambda}^L(\mathbf{r}) a_{\mathbf{k}\lambda}^L e^{-i\omega_{\mathbf{k}}t} \\ &\quad \left. + \int d^2\mathbf{k}_\parallel \sum_{k_{z1}} \frac{1}{\sqrt{2\epsilon_0\omega_{\mathbf{k}}}} \mathbf{f}_{\mathbf{k}\lambda}^T(\mathbf{r}) a_{\mathbf{k}\lambda}^T e^{-i\omega_{\mathbf{k}}t} \right\} + \text{H.C.} \quad (36) \end{aligned}$$

The sum in the last term runs over the allowed values of the z -component of the layer's wave vector k_{z1} , i.e. the solutions of the dispersion relation (32). For a given

type of mode, left-incident, right-incident, or trapped, photon creation and annihilation operators appearing in (36) satisfy the commutation relations (10). Commutators between photon operators corresponding to different types of modes vanish as a consequence of the orthogonality of the field modes (8), e.g.

$$\left[a_{\mathbf{k}\lambda}^L, (a_{\mathbf{k}'\lambda'}^R)^\dagger \right] = 0. \quad (37)$$

We would like to verify explicitly the equal-time canonical commutation relation between field operators, say, between the electric field operator $\hat{\mathbf{E}}(\mathbf{r}, t)$ and the vector potential operator $\hat{\mathbf{A}}(\mathbf{r}, t)$

$$\left[\hat{A}_i(\mathbf{r}, t), \epsilon_0 \hat{E}_j(\mathbf{r}', t) \right] = -i\delta_{ij}^\epsilon(\mathbf{r}, \mathbf{r}'), \quad z, z' > L/2 \quad (38)$$

with $\delta_{ij}^\epsilon(\mathbf{r}, \mathbf{r}')$ given by Eq. (6) and (7). To evaluate (38) we shall need the electric field operator which is easily obtained from Eq. (36) using the relation $\mathbf{E} = -\partial_t \mathbf{A}$. Plugging in the field operators into (38) and making use of commutation relations (10) and (37), we find that the LHS of (38) is given by

$$\begin{aligned} \text{LHS} = i\text{Re} \sum_{\lambda} \int d^2 \mathbf{k}_{\parallel} & \left[\int_0^{\infty} dk_z f_{\mathbf{k}\lambda, i}^R(\mathbf{r}) f_{\mathbf{k}\lambda, j}^{*R}(\mathbf{r}') \right. \\ & + \int_0^{\infty} dk_{zs} f_{\mathbf{k}\lambda, i}^L(\mathbf{r}) f_{\mathbf{k}\lambda, j}^{*L}(\mathbf{r}') \\ & \left. + \sum_{k_{z1}} f_{\mathbf{k}\lambda, i}^T(\mathbf{r}) f_{\mathbf{k}\lambda, j}^{*T}(\mathbf{r}') \right]. \quad (39) \end{aligned}$$

The quantity on the right-hand side is the sum over all modes, just as prescribed by equation (5), and therefore we expect it to be equal to the generalized transverse delta function, Eq. (6). This shows that the statement of the completeness of the modes (5) is in fact equivalent to the commutation relation (38), as has been noted before in [18]. To prove that the relation

$$\begin{aligned} \delta_{ij}^\epsilon(\mathbf{r}, \mathbf{r}') = \sum_{\lambda} \int d^2 \mathbf{k}_{\parallel} & \left[\int_0^{\infty} dk_z f_{\mathbf{k}\lambda, i}^R(\mathbf{r}) f_{\mathbf{k}\lambda, j}^{*R}(\mathbf{r}') \right. \\ & + \int_0^{\infty} dk_{zs} f_{\mathbf{k}\lambda, i}^L(\mathbf{r}) f_{\mathbf{k}\lambda, j}^{*L}(\mathbf{r}') \\ & \left. + \sum_{k_{z1}} f_{\mathbf{k}\lambda, i}^T(\mathbf{r}) f_{\mathbf{k}\lambda, j}^{*T}(\mathbf{r}') \right] \quad (40) \end{aligned}$$

holds for $z, z' > L/2$ we need to work out the sum over all field modes. To start with we carry out a change of variables in (40): we convert the k_{zs} -integral and the k_{z1} -sum to run over the values of k_z . In the case of the k_{zs} -integral this is a simple change of variables according to (17)

$$\int_0^{\infty} dk_{zs} = n_s^2 \int_0^{\infty} dk_z \frac{k_z}{k_{zs}} + n_s^2 \int_{i\Gamma_s}^0 dk_z \frac{k_z}{k_{zs}} \quad (41)$$

with $\Gamma_s = \sqrt{(n_s^2 - 1)\mathbf{k}_{\parallel}^2}/n_s$. Here it is seen explicitly that the contributions from the left-incident modes split into

a travelling part and an evanescent part. The values of k_z included in the last integral correspond to the condition for evanescent modes with continuous spectrum, Eq. (27). In the case of the sum we change the summation over k_{z1} to run over the values of k_z as defined by equation (33). Plugging in the mode functions (20) and (21) into equation (40) and utilizing straightforward properties of the reflection and transmission coefficients that hold for real k_z, k_{zs} ,

$$R_{\lambda}^{*R}(-k_z) = R_{\lambda}^R(k_z), \quad \frac{k_z}{k_{zs}} |T_{\lambda}^L|^2 + |R_{\lambda}^R|^2 = 1, \quad (42)$$

we can rewrite the completeness relation as

$$\begin{aligned} \delta_{ij}^\epsilon(\mathbf{r}, \mathbf{r}') = \delta_{ij}^{\perp}(\mathbf{r} - \mathbf{r}') \\ + \sum_{\lambda} \hat{e}_{\lambda}^i(\nabla) \hat{e}_{\lambda}^{*j}(\nabla') \int d^2 \mathbf{k}_{\parallel} e^{i\mathbf{k}_{\parallel}(\mathbf{r}_{\parallel} - \mathbf{r}'_{\parallel})} \\ \times \left\{ \sum_{q_{\lambda}^n} |N_{\lambda}|^2 |T_{\lambda}^{\perp}|^2 e^{ik_z(z+z')} \right. \\ \left. + \frac{1}{(2\pi)^3} \int_{i\Gamma_s}^0 dk_z \frac{k_z}{k_{zs}} |T_{\lambda}^L|^2 e^{ik_z(z+z')} \right. \\ \left. + \frac{1}{(2\pi)^3} \int_{-\infty}^0 dk_z R_{\lambda}^R e^{ik_z(z+z')} \right\}. \quad (43) \end{aligned}$$

The first term in the above equation is the standard transverse delta-function. Therefore, if equation (40) is to hold, the term in the curly brackets needs to be proportional to the reflection part of the electrostatic Green's function, cf. the second term on the RHS of Eq. (7). That this is indeed the case is at this stage far from obvious, as for the proof one would need to combine two integrals and a sum into one expression. Obviously, the discreteness of the spectrum of the trapped modes is a nuisance that needs to be overcome if one is to complete the task of summing over the electromagnetic modes successfully. A similar difficulty would arise in any perturbative calculation in this type of geometry, which motivated a previous investigation of this problem for the symmetric case of a single slab of dielectric material [17]. We proceed with a broadly analogous method to [17], first noting that what we have here can be considered as a superposition of a slab and a half-space geometry, cf. [17] and [18]. One can utilize the branch-cut due to k_{zs} (which runs along the imaginary k_z axis between $\pm i\Gamma_s$, cf. Fig. 2) to express the integral over $|T_{\lambda}^L|^2$ in (43) as an integral over the reflection coefficient R_{λ}^R that runs from 0^- along the square root cut up to the branch-point at $+i\Gamma_s$ and then back down to the origin 0^+ . Note that the branch-cut due to the k_{z1} is irrelevant because of the symmetry property of the reflection coefficient $R_{\lambda}^R(-k_{z1}) = R_{\lambda}^R(k_{z1})$. In this way, the first two integrals in the curly braces in equation (43) can be combined together as a single integral in the complex k_z plane [18]. This is possible because the relation

$$\frac{k_z}{k_{zs}} |T_{\lambda}^L|^2 \Big|_{k_{zs}, k_{z1} > 0} = R_{\lambda}^R \Big|_{k_{zs}, k_{z1} > 0} - R_{\lambda}^R \Big|_{k_{zs}, k_{z1} < 0} \quad (44)$$

continues to hold for coefficients (22) with a purely imaginary z -component of the vacuum wave vector, k_z (cf. [19]). Thus, the contributions from the travelling and evanescent modes can be combined into a single contour integral along the path γ_s depicted in Fig. 2 and the terms appearing in the curly brackets on the RHS of Eq. (43) become

$$\frac{1}{(2\pi)^3} \int_{\gamma_s} dk_z R_\lambda^R \hat{e}_\lambda^i(\mathbf{k}^+) \hat{e}_\lambda^j(\mathbf{k}^-) e^{ik_z(z+z')} + \sum_{q_\lambda^n} |N_\lambda|^2 |T_\lambda^{lv}|^2 \hat{e}_\lambda^i(\mathbf{k}^+) \hat{e}_\lambda^j(\mathbf{k}^-) e^{ik_z(z+z')}. \quad (45)$$

Here we have now included the polarization vectors explicitly in the integrals, which is a crucial step as they affect the analytical structure of the integrand in the complex k_z -plane. In particular, the TM polarization vector introduces a pole at the points $k_z = \pm i|\mathbf{k}_\parallel|$ due to the factor $1/|\mathbf{k}|^2$ in its normalization factor. We will see that it is precisely this pole that gives rise to the reflection term in (6). We note that, according to Eq. (22), the reflec-

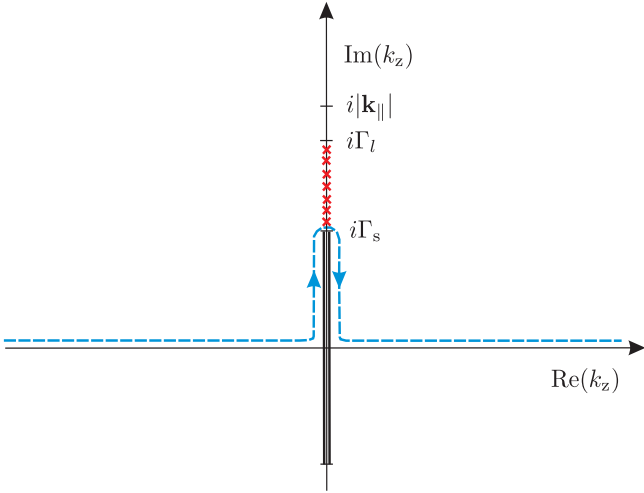


FIG. 2: The dashed line represents the contour γ_s used to evaluate the k_z integral in Eq. (45). Here $\Gamma_s = \sqrt{(n_s^2 - 1)\mathbf{k}_\parallel^2}/n_s$ and $\Gamma_l = \sqrt{(n_l^2 - 1)\mathbf{k}_\parallel^2}/n_l$. The crosses represent the poles of the reflection coefficient R_λ^R i.e. the solutions to the dispersion relation (32).

tion coefficient contains the phase factor $e^{-ik_z L}$. Thus, since $z + z' - L > 0$, the argument of the exponential in (45) has a negative real part in the upper half of the complex k_z plane and we can evaluate the k_z -integral in Eq. (45) by closing the contour in the upper half-plane. For this we need to determine the analytical properties of R_λ^R . We note that the denominator of the reflection coefficient (22) is precisely the dispersion relation (32).

Rewriting the reflection coefficients in the form

$$R_{\text{TE}}^R = \frac{k_z - k_{z1} \left(\frac{1 - r_{\text{TE}}^{\text{ls}} \exp(2ik_{z1}L)}{1 + r_{\text{TE}}^{\text{ls}} \exp(2ik_{z1}L)} \right)}{k_z + k_{z1} \left(\frac{1 - r_{\text{TE}}^{\text{ls}} \exp(2ik_{z1}L)}{1 + r_{\text{TE}}^{\text{ls}} \exp(2ik_{z1}L)} \right)},$$

$$R_{\text{TM}}^R = \frac{k_z - \frac{k_{z1}}{n_1^2} \left(\frac{1 - r_{\text{TM}}^{\text{ls}} \exp(2ik_{z1}L)}{1 + r_{\text{TM}}^{\text{ls}} \exp(2ik_{z1}L)} \right)}{k_z + \frac{k_{z1}}{n_1^2} \left(\frac{1 - r_{\text{TM}}^{\text{ls}} \exp(2ik_{z1}L)}{1 + r_{\text{TM}}^{\text{ls}} \exp(2ik_{z1}L)} \right)},$$

allows us to deduce that R_λ^R has a finite number of simple poles on the imaginary axis. When closing the contour we enclose all of them and by Cauchy's theorem the problem is reduced to the evaluation of the residues at these points:

$$\sum_\lambda \int_{\gamma_s} dk_z R_\lambda^R \hat{e}_\lambda^i(\mathbf{k}^+) \hat{e}_\lambda^j(\mathbf{k}^-) e^{ik_z(z+z')} = 2\pi i \sum_\lambda \sum_{\text{Res}} R_\lambda^R \hat{e}_\lambda^i(\mathbf{k}^+) \hat{e}_\lambda^j(\mathbf{k}^-) e^{ik_z(z+z')} = 2\pi i \left[\sum_\lambda \sum_{q_\lambda^n} \lim_{k_z \rightarrow q_\lambda^n} (k_z - q_\lambda^n) + \lim_{k_z \rightarrow i|\mathbf{k}_\parallel|} (k_z - i|\mathbf{k}_\parallel|) \right] \times \hat{e}_\lambda^i(\mathbf{k}^+) \hat{e}_\lambda^j(\mathbf{k}^-) \frac{r_\lambda^{v1} + r_\lambda^{\text{ls}} e^{2ik_{z1}L}}{1 + r_\lambda^{v1} r_\lambda^{\text{ls}} e^{2ik_{z1}L}} e^{ik_z(z+z'-L)} \quad (46)$$

Here, the first term represents the contributions from the poles in the reflection coefficient and corresponds the trapped modes, whereas the second term represents the contribution from the pole that arises due to the TM polarization vector. When calculating the residues explicitly one needs to remember that the two independent variables are k_z and \mathbf{k}_\parallel and that, according to Eq. (16) and (17), k_{z1} and k_{zs} are functions of those. In addition, the denominator of the reflection coefficient is not of the form $f(k_z)(k_z - q_\lambda^n)$ so that multiplying it by $(k_z - q_\lambda^n)$ does not remove its singularity; the whole expression is still indeterminate. Therefore, L'Hospital's rule needs to be used to evaluate the limit (cf.[17, Section V]). Doing so, we find that

$$\frac{1}{(2\pi)^3} \int_{\gamma_s} dk_z R_\lambda^R \hat{e}_\lambda^i(\mathbf{k}^+) \hat{e}_\lambda^j(\mathbf{k}^-) e^{ik_z(z+z')} = - \sum_{q_\lambda^n} |N_\lambda|^2 |T_\lambda^{lv}|^2 \hat{e}_\lambda^i(\mathbf{k}^+) \hat{e}_\lambda^j(\mathbf{k}^-) e^{ik_z(z+z')} - \nabla_i \nabla_j' G_H(\mathbf{r}, \mathbf{r}') \quad (47)$$

where $G_H(\mathbf{r}, \mathbf{r}')$ is the reflected part of the Green's function of the Poisson equation given in Eq. (7) and derived in Appendix B. We see that the poles of the reflection coefficient R_λ^R yield a term that exactly cancels out the contributions of the trapped modes to the completeness relation (43) whereas the pole of the TM polarization vector yields the term proportional to Green's function.

Thus, the final result can be written as

$$\begin{aligned} \int d^2\mathbf{k}_{\parallel} \sum_{k_z}^{\neq} f_{\mathbf{k}\lambda}^i(\mathbf{r}) f_{\mathbf{k}\lambda}^{*j}(\mathbf{r}') &= \frac{1}{i} [A_i(\mathbf{r}), -\epsilon_0 E_j(\mathbf{r}')] \\ &= \delta_{ij}^{\perp}(\mathbf{r} - \mathbf{r}') - \nabla_i \nabla_j' G_H(\mathbf{r}, \mathbf{r}') \quad z, z' > L/2 \\ &= \delta_{ij}^{\perp} \delta^{(3)}(\mathbf{r} - \mathbf{r}') - \nabla_i \nabla_j' G(\mathbf{r}, \mathbf{r}') \quad z, z' > L/2 \end{aligned}$$

which is precisely what we have anticipated earlier. In the next section we demonstrate how the calculation presented here may be applied to accomplish typical perturbative QED calculations in a layered geometry.

III. ENERGY SHIFT

To work out the energy shift we use standard perturbation theory where the atom is treated by means of the Schrödinger quantum mechanics and only the electromagnetic field is second-quantized. We work with a multipolar coupling where the lowest order of the interaction Hamiltonian is

$$H_{\text{int}} = -\boldsymbol{\mu} \cdot \mathbf{E}. \quad (48)$$

Then the energy shift of the atomic state i , up to the second-order, is given by

$$\Delta E_i = \langle i; 0 | H_{\text{int}} | i; 0 \rangle + \sum_{j \neq i} \sum_{\mathbf{k}, \lambda} \frac{|\langle j; 1_{\mathbf{k}\lambda} | H_{\text{int}} | i; 0 \rangle|^2}{E_i - (E_j + \omega_{\mathbf{k}})}.$$

Here, $\boldsymbol{\mu}$ is the atomic electric dipole moment, and the composite state $|j; 1_{\mathbf{k}\lambda}\rangle$ describes the atom in the state $|j\rangle$ with energy E_j and the photon field containing one photon with momentum \mathbf{k} and polarization λ . Because the electric field operator is linear in the photon creation and annihilation operators, the first-order contribution vanishes and the second-order correction is the lowest-order contribution. Since the electric field does not vary appreciably over the size of the atom we use the electric dipole approximation. Then the energy shift can be expressed as

$$\Delta E_i = - \sum_{j \neq i} \sum_{\mathbf{k}, \lambda} \frac{\omega_{\mathbf{k}} |\langle i | \boldsymbol{\mu} | j \rangle \cdot \mathbf{f}_{\mathbf{k}\lambda}^*(\mathbf{r}_0)|^2}{2\epsilon_0 (E_j + \omega_{\mathbf{k}})} \quad (49)$$

where $\mathbf{r}_0 = (0, 0, z_0)$ is the position of the atom and we have abbreviated $E_{ji} = E_j - E_i$. It is seen that the calculation involves a summation over the modes of the electromagnetic field as carried out in the proof of the completeness relation (43). Equation (49) can be written out explicitly as

$$\begin{aligned} \Delta E_i &= -\frac{1}{2\epsilon_0} \sum_{\lambda} \sum_{j \neq i} |\mu_m|^2 \int d\mathbf{k}_{\parallel} \\ &\quad \times (\Delta^{\text{vac}} + \Delta^{\text{trav}} + \Delta^{\text{evan}} + \Delta^{\text{trap}}) \quad (50) \end{aligned}$$

with $|\mu_m|^2 \equiv |\langle i | \mu_m | j \rangle|^2$. There are four distinct contributions to the energy shift. Δ^{vac} is the position-independent contribution caused by the vacuum fields and gives rise to the Lamb shift in free space

$$\Delta^{\text{vac}} = \frac{1}{(2\pi)^3} \int_{-\infty}^{\infty} dk_z e_{\lambda}^m(\mathbf{k}^-) e_{\lambda}^{m*}(\mathbf{k}^-) \frac{\omega}{E_{ji} + \omega}. \quad (51)$$

The remaining three contributions come from the travelling, evanescent, and trapped modes, respectively,

$$\begin{aligned} \Delta^{\text{trav}} &= \frac{1}{(2\pi)^3} \int_{-\infty}^{\infty} dk_z R_{\lambda}^R e_{\lambda}^m(\mathbf{k}^+) e_{\lambda}^{m*}(\mathbf{k}^-) e^{2ik_z z_0} \frac{\omega}{E_{ji} + \omega}, \\ \Delta^{\text{evan}} &= \frac{1}{(2\pi)^3} \int_{i\Gamma_s}^0 dk_z \frac{k_z}{k_{zs}} |T_{\lambda}^L|^2 e_{\lambda}^m(\mathbf{k}^+) e_{\lambda}^{m*}(\mathbf{k}^+) e^{2ik_z z_0} \\ &\quad \times \frac{\omega}{E_{ji} + \omega}, \quad (52) \\ \Delta^{\text{trap}} &= \sum_{q_{\lambda}^n} |N_{\lambda}|^2 |T_{\lambda}^{\text{lv}}|^2 e_{\lambda}^m(\mathbf{k}^+) e_{\lambda}^{m*}(\mathbf{k}^+) e^{2ik_z z_0} \frac{\omega}{E_{ji} + \omega}, \end{aligned}$$

with z_0 being the position of the atom with respect to the origin. Note that because of the dipole approximation the shorthand notation for polarisation vectors (19) can be no longer applied. Normally one is interested in the energy shift caused by the presence of the dielectric boundaries only i.e. the correction to the shift that would appear in the free space. Therefore, we renormalize the energy-level shift (50) by subtracting from it its free space limit, i.e.

$$\Delta E_i^{\text{ren}} = \Delta E_i - \lim_{n_1, n_s \rightarrow 1} \Delta E_i. \quad (53)$$

The renormalization procedure amounts to the removal of the contributions Δ^{vac} , Eq. (51), from the energy shift (50) and takes care of any infinities that would appear otherwise, provided we treat the remaining parts with care. As noted elsewhere [1], the contributions (52) suffer from convergence problems when treated separately. However, appropriate tools to handle the problem have been developed in Sec. II C. We aim to combine Δ^{trav} , Δ^{evan} and Δ^{trap} into one compact expression that is easy to handle analytically. We can use the same trick as in the proof of the completeness relation because the analytical structure of the integrand in the complex k_z -plane is the same except for the function $\omega = (\mathbf{k}_{\parallel}^2 + k_z^2)^{1/2}$ that comes about due to the denominator of perturbation theory and introduces additional branch-points at $k_z = \pm i|\mathbf{k}_{\parallel}|$ as compared to Fig. 2. This poses no difficulties though, if one chooses the branch-cuts to lie between $\pm i|\mathbf{k}_{\parallel}|$ and $\pm i\infty$. Then, the contributions to the energy shift from the travelling modes Δ^{trav} and the evanescent modes Δ^{evan} can be combined together into a single complex integral as explained in the steps between Eq. (43) and Eq. (45). This is possible because for imaginary k_z we have $e_{\lambda}^{m*}(\mathbf{k}^+) = e_{\lambda}^m(\mathbf{k}^-)$, whereas for real k_z the relation $e_{\lambda}^{m*}(\mathbf{k}^-) = e_{\lambda}^m(\mathbf{k}^-)$ holds. On the other hand, we also know from Eq. (47) that the sum in Δ^{trap} is equal to an integral over the reflection coefficient R_{λ}^R taken along

any clockwise contour enclosing all of it's poles. Choosing this contour to run from $k_z = 0^- + i\Gamma_s$ to $k_z = 0^- + i\Gamma_1$ and then back down from $k_z = 0^+ + i\Gamma_1$ to $k_z = 0^+ + i\Gamma_s$, cf. Fig. 3, we write down the renormalized energy shift compactly as

$$\Delta E_i^{\text{ren}} = -\frac{1}{2(2\pi)^3\epsilon_0} \sum_{m,\lambda} \sum_{j \neq i} |\mu_m|^2 \int d\mathbf{k}_{\parallel} \times \int_{\gamma_1} dk_z \frac{\omega}{E_{ji} + \omega} R_{\lambda}^R e_{\lambda}^m(\mathbf{k}^+) e_{\lambda}^m(\mathbf{k}^-) e^{2ik_z z_0} \quad (54)$$

where the contour of integration γ_1 is shown in Fig. 3. It resembles that of Fig. 2 but now runs on the imaginary axis up to the point $k_z = i\Gamma_1$ enclosing all the poles of the reflection coefficients R_{λ}^R . Formula (54) is equally

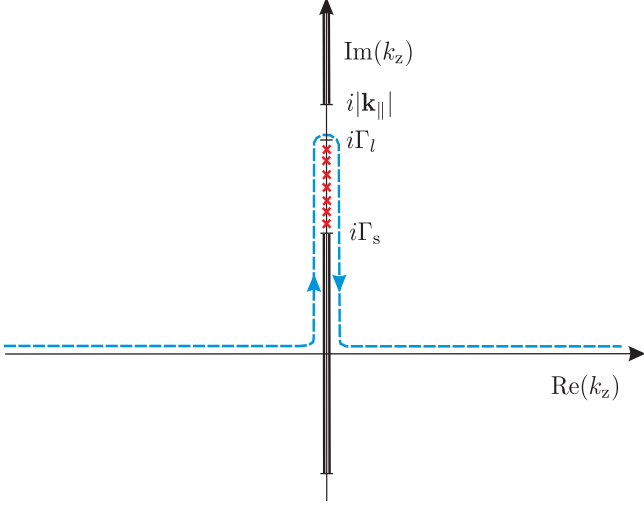


FIG. 3: The dashed line represents the final contour γ_1 used to evaluate the energy shift in Eq. (54).

applicable to ground-state atoms $|0\rangle$ as it is to atoms that are in an excited state $|i\rangle$ provided we use the contour of integration as given in Fig. 3 and interpret the k_z integral as a Cauchy principal-value. As renormalization has now been dealt with we shall from now on omit the superscript “ren” and designate the renormalized energy shift of Eq. (54) simply by ΔE_i .

A. Ground state atoms

In the case of a ground-state atom the energy difference $E_{j0} \equiv E_j - E_0$ is always positive hence the denominator in Eq. (54) that originates from second-order perturbation theory, $E_{j0} + \omega$, never vanishes. Then, Eq. (54) contains no poles in the upper half of the k_z -plane other than those due to the reflection coefficient R_{λ}^R . To evaluate the k_z integral we can deform the contour of integration in Eq. (54) from that sketched in Fig. 3 to the one as shown in Fig. 4 which is beneficial from the computational point of view as it simplifies the analysis of Eq. (54) considerably. Writing out explicitly

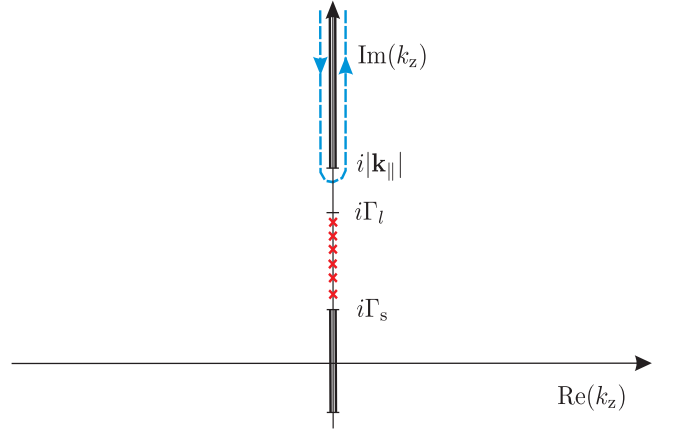


FIG. 4: The final contour \mathcal{C} used to evaluate the energy shift of the ground state atom in Eq. (55).

the sums over the polarization vectors (19) and then expressing the integral in the \mathbf{k}_{\parallel} -plane in polar coordinates, $k_x = k_{\parallel} \cos \phi$, $k_y = k_{\parallel} \sin \phi$, where the angle integral is computable analytically, we rewrite the energy shift as

$$\Delta E_0 = \frac{1}{16\pi^2\epsilon_0} \sum_{j \neq 0} \int_0^{\infty} dk_{\parallel} k_{\parallel} \int_{\mathcal{C}} dk_z \frac{\omega}{E_{j0} + \omega} e^{2ik_z z} \times \left[|\mu_{\parallel}|^2 \left(\tilde{R}_{\text{TE}}^R - \frac{k_z^2}{\omega^2} \tilde{R}_{\text{TM}}^R \right) + 2|\mu_{\perp}|^2 \frac{k_{\parallel}^2}{\omega^2} \tilde{R}_{\text{TM}}^R \right] \quad (55)$$

with $\omega(k_z) = \sqrt{k_{\parallel}^2 + k_z^2}$, $|\mu_{\parallel}|^2 = |\mu_x|^2 + |\mu_y|^2$ and the contour \mathcal{C} is that in Fig. 4. The amended reflection coefficients \tilde{R}_{λ}^R are given by

$$\tilde{R}_{\lambda}^R = \frac{r_{\lambda}^{\text{vl}} + r_{\lambda}^{\text{ls}} e^{2ik_z L}}{1 + r_{\lambda}^{\text{vl}} r_{\lambda}^{\text{ls}} e^{2ik_z L}}, \quad (56)$$

i.e. we have pulled out the phase factor $e^{-ik_z L}$ in order to define $\mathcal{Z} = z_0 - L/2$ as the distance between the atom and the surface, cf. Eq. (22).

In order to perform the k_z integration in (55) we need to analytically continue the function $\omega = \omega(k_z)$, which is real and positive on the real axis, to the both sides of the branch cut along which the integration is carried out, (cf. Fig. 4). Doing so we find that on the LHS of the cut the positive value of the square root needs to be taken, and hence on the RHS of the cut we must take the opposite sign. Therefore we have

$$\int_{\mathcal{C}} dk_z \frac{\omega}{E_{j0} + \omega} = - \int_{iq}^{i\infty} dk_z \frac{2E_{j0}\omega}{(E_{j0} - \omega)(E_{j0} + \omega)}.$$

Now we carry out a sequence of changes of variables. First we re-express the k_z integration in terms of one over the frequency ω by substituting $\omega = \sqrt{k_{\parallel}^2 + k_z^2}$,

$$\int_{ik_{\parallel}}^{i\infty} dk_z = \int_0^{i\infty} d\omega \frac{\omega}{\sqrt{\omega^2 - k_{\parallel}^2}}. \quad (57)$$

Then, we make the integral run along the real axis by setting $\omega = i\xi$. After this is done, the energy shift of the ground state is expressed as a double integral that covers the first quadrant of the (k_{\parallel}, ξ) -plane

$$\Delta E_0 = -\frac{1}{8\pi^2\epsilon_0} \sum_{j \neq i} E_{j0} \int_0^\infty dk_{\parallel} k_{\parallel} \int_0^\infty d\xi \frac{e^{-2\sqrt{\xi^2 + k_{\parallel}^2} z}}{\sqrt{\xi^2 + k_{\parallel}^2} (E_{j0}^2 + \xi^2)} \times \left\{ |\mu_{\parallel}|^2 \left[(\xi^2 + k_{\parallel}^2) \tilde{R}_{\text{TM}}^R - \xi^2 \tilde{R}_{\text{TE}}^R \right] + 2k_{\parallel}^2 \tilde{R}_{\text{TM}}^R |\mu_{\perp}|^2 \right\}.$$

It seems natural to introduce polar coordinates, $k_{\parallel} = \bar{x} \sin \phi$, $\xi = \bar{x} \cos \phi$. We also choose to scale the radial integration variable $\bar{x} = E_{j0} x$ with $E_{j0} > 0$ and set $y = \cos \phi$. This provides us with the final form of the energy shift that is more suitable for numerical computations and asymptotic analysis

$$\Delta E_0 = \frac{1}{8\pi^2\epsilon_0} \sum_{j \neq i} E_{j0}^3 \int_0^\infty dx x^3 \int_0^1 dy \frac{e^{-2E_{j0} z x}}{1 + x^2 y^2} \times \left[|\mu_{\parallel}|^2 \left(y^2 \tilde{R}_{\text{TE}}^R - \tilde{R}_{\text{TM}}^R \right) + 2|\mu_{\perp}|^2 (y^2 - 1) \tilde{R}_{\text{TM}}^R \right]. \quad (58)$$

The reflection coefficients \tilde{R}_{λ}^R are as expressed in (56) but with the wave vectors given by

$$k_{zi} = ix E_{j0} \sqrt{(n_i^2 - 1)y^2 + 1}, \quad n_i = \{1, n_1, n_s\}.$$

Note that even though the wave vector is imaginary, the final result is a real number, as it should, because the Fresnel coefficients contain only ratios of wave vectors.

B. Excited atoms

As mentioned previously, the energy-level shift of an excited atom is also given by Eq. (54). However, one needs to take account of the fact that the quantity $E_{ji} \equiv E_j - E_i$ can now become negative for $E_j < E_i$, so that the denominator originating from perturbation theory contributes additional poles lying on the path of k_z integration, shown in Fig. 3 and is now to be understood as a Cauchy principal-value. These poles are located at $k_z = \pm \sqrt{E_{ji}^2 - \mathbf{k}_{\parallel}^2}$, though their precise location depends on the value of $|\mathbf{k}_{\parallel}|$ that is not fixed but varies as we carry out the \mathbf{k}_{\parallel} integrations in equation (54). For $|\mathbf{k}_{\parallel}| \in [0, |E_{ji}|]$ the poles are located on the real k_z axis but as we increase the value of $|\mathbf{k}_{\parallel}|$ to exceed $|E_{ji}|$ both poles move onto the positive imaginary axis according to the convention that $\text{Im}(k_z) > 0$. For $|\mathbf{k}_{\parallel}|$ belonging to the interval $[|E_{ji}|, n_s |E_{ji}|]$ the poles are located on the opposite sides of the branch-cut due to the k_{zs} and care needs to be taken when evaluating those pole contributions. To evaluate the Cauchy principal-value of the k_z -integral we circumvent the poles and close the contour in the upper half-plane, as was done in the previous section. The contribution from the large semicircle vanishes and equation

(54) acquires pole contributions that are easily worked out by the residue theorem. The energy shift splits into the "non-resonant" ground-state-like part ΔE_i and a "resonant" oscillatory part ΔE_i^{res} that arises only if the atom is in an excited state. In analogy to the result of the previous section, the "non-resonant" part is given by

$$\Delta E_i = \frac{1}{8\pi^2\epsilon_0} \sum_{j \neq i} E_{ji}^3 \int_0^\infty dx x^3 \int_0^1 dy \frac{e^{-2|E_{ji}| z x}}{1 + x^2 y^2} \times \left[|\mu_{\parallel}|^2 \left(y^2 \tilde{R}_{\text{TE}}^R - \tilde{R}_{\text{TM}}^R \right) + 2|\mu_{\perp}|^2 (y^2 - 1) \tilde{R}_{\text{TM}}^R \right] \quad (59)$$

with wave vectors expressed as

$$k_{zi} = ix |E_{ji}| \sqrt{(n_i^2 - 1)y^2 + 1}, \quad n_i = \{1, n_1, n_s\}, \quad (60)$$

whereas the "resonant" part is given by

$$\Delta E_i^{\text{res}} = \text{Re} \frac{i}{8\pi\epsilon_0} \sum_{j < i} |E_{ji}|^3 \int_0^\infty \frac{dq q}{\sqrt{1 - q^2}} e^{2i|E_{ji}| \sqrt{1 - q^2} z} \times \left\{ |\mu_{\parallel}|^2 \left[(1 - q^2) \tilde{R}_{\text{TM}}^R - \tilde{R}_{\text{TE}}^R \right] - 2|\mu_{\perp}|^2 q^2 \tilde{R}_{\text{TM}}^R \right\}, \quad (61)$$

with wave vectors expressed as

$$k_{zi} = |E_{ji}| \sqrt{n_i^2 - q^2}, \quad n_i = \{1, n_1, n_s\}.$$

The reflection coefficients are as given in (56). The integral in Eq. (61) contains poles because the dispersion relation present in the denominators of the reflection coefficients has now solutions on the real axis when $q \in [n_s, n_1]$. This signals contributions from surface excitations (trapped modes). This fact has been mentioned in [2] where the interaction of an excited atom with layered dielectric has been studied, although using mainly numerical analysis. Here we will attempt to study the results (59) and (61) analytically. To do so it will prove beneficial to rewrite equation (61) slightly. We change variables according to $\sqrt{1 - q^2} = \eta$ and split the contributions to Eq. (61) into two parts. The first one is a contribution from the travelling modes and given by

$$\Delta E_i^{\text{res, trav}} = -\text{Re} \frac{i}{8\pi\epsilon_0} \sum_{j < i} |E_{ji}|^3 \int_0^1 d\eta e^{2i|E_{ji}| z \eta} \times \left\{ |\mu_{\parallel}|^2 \left[\tilde{R}_{\text{TE}}^R - \eta^2 \tilde{R}_{\text{TM}}^R \right] + 2|\mu_{\perp}|^2 (1 - \eta^2) \tilde{R}_{\text{TM}}^R \right\} \quad (62)$$

where the wave vectors in reflection coefficients are all real and can be expressed as

$$k_{zi} = |E_{ji}| \sqrt{n_i^2 - 1 + \eta^2}, \quad n_i = \{1, n_1, n_s\}, \quad (63)$$

and the second is a contribution from the evanescent modes

$$\Delta E_i^{\text{res, evan}} = -\text{Re} \frac{1}{8\pi\epsilon_0} \sum_{j < i} |E_{ji}|^3 \int_0^\infty d\eta e^{-2|E_{ji}| z \eta} \times \left\{ |\mu_{\parallel}|^2 \left[\tilde{R}_{\text{TE}}^R + \eta^2 \tilde{R}_{\text{TM}}^R \right] + 2|\mu_{\perp}|^2 (1 + \eta^2) \tilde{R}_{\text{TM}}^R \right\} \quad (64)$$

where the wave vectors in reflection coefficients can be expressed as

$$k_{zi} = |E_{ji}| \sqrt{n_i^2 - 1 - \eta^2}, \quad n_i = \{1, n_1, n_s\}. \quad (65)$$

Finally, it is worth noting that the imaginary part of Eq. (61) is actually proportional to the modified decay rates [9]. These have already been studied in [16] so that we focus on energy shifts only. However, the methods of analysis that are reported in the next section do allow one to write down at once equivalent analytical formulae for the decay rates.

IV. ASYMPTOTIC ANALYSIS

The interaction between the atom and the dielectric is electromagnetic in nature and it is mediated by photons. The atomic system in state $|i\rangle$ evolves in time with a characteristic time-scale that is proportional to E_{ji}^{-1} , with E_{ji} being the energy-level spacing between the states $|i\rangle$ and $|j\rangle$ which are connected by the strongest dipole transition from state $|i\rangle$. Since it takes a finite time for the photon to make a round trip between the atom and the surface, the atom will have changed by the time the photon comes back. Therefore, the ratio of the time needed by the photon to travel to the surface and back and the typical time-scale of atomic evolution is a fundamental quantity that plays decisive role in characterising the interaction. In natural units, if $2E_{ji}\mathcal{Z} \ll 1$ we can safely assume that the interaction is instantaneous and we are in the so-called non-retarded or van der Waals regime. If $2E_{ji}\mathcal{Z} \gg 1$ the interaction becomes manifestly retarded as the atom will have changed significantly by the time the photon comes back. However, the problem we have considered here provides us with yet another length scale, namely the thickness of the top layer L . We shall now consider the energy shift in various asymptotic regimes.

A. Ground state atoms. Electrostatic limit, ($2E_{ji}\mathcal{Z} \ll 1$)

In this limit the interaction is instantaneous (or electrostatic) in nature and the energy shift is obtainable using the Green's function of the classical Laplace equation (cf. e.g. [20]). This classical derivation is outlined in the Appendix B. The end result for the energy shift reads

$$\Delta E^{\text{el}} = -\frac{1}{16\pi\epsilon_0} \left(\langle \mu_{\parallel}^2 \rangle + 2\langle \mu_{\perp}^2 \rangle \right) \int_0^{\infty} dk k^2 e^{-2kz} \times \left(\frac{\frac{n_1^2 - 1}{n_1^2 + 1} - \frac{n_1^2 - n_s^2}{n_s^2 + n_1^2} e^{-2kL}}{1 - \frac{n_1^2 - 1}{n_1^2 + 1} \frac{n_1^2 - n_s^2}{n_s^2 + n_1^2} e^{-2kL}} \right), \quad (66)$$

with $\langle \mu_{\parallel}^2 \rangle \equiv \langle \mu_x^2 \rangle + \langle \mu_y^2 \rangle$ and $\langle \mu_{\perp}^2 \rangle \equiv \langle \mu_z^2 \rangle$. We will now show that one can also obtain the above result as a limiting case of the results of previous section, thus providing a cross-check for our general calculation. To start with we note that equation (58) cannot be used to take the electrostatic limit in which we mathematically let $E_{ji} \rightarrow 0$ because it has been scaled with E_{ji} . Therefore, it is best to start from equation (54). The result of Eq. (66) can be derived very quickly if we observe that in the limit $E_{ji} \rightarrow 0$ the branch cut due to $\omega = \sqrt{\mathbf{k}_{\parallel}^2 + k_z^2}$ is no longer present and the contour in Fig. 4 collapses to a simple enclosure of the point $k_z = i|\mathbf{k}_{\parallel}|$. The contribution from the TE mode vanishes as the product of the polarization vectors is regular at $k_z = i|\mathbf{k}_{\parallel}|$, but for the TM mode this point is a simple pole, cf. Eq. (19). Therefore we obtain

$$\Delta E^{\text{el}} = -\frac{1}{(2\pi)^3 2\epsilon_0} \sum_m \sum_{j \neq i} |\mu_m|^2 \int d\mathbf{k}_{\parallel} \times 2\pi i \lim_{k_z \rightarrow i|\mathbf{k}_{\parallel}|} (k_z - i|\mathbf{k}_{\parallel}|) R_{\text{TM}}^R e_{\text{TM}}^m(\mathbf{k}^+) e_{\text{TM}}^m(\mathbf{k}^-) e^{2ik_z z_0}.$$

Taking the limit and expressing the remaining integrals in polar coordinates, where the angle integral is elementary, yields equation (66) with $\langle \mu_m^2 \rangle \equiv \sum_{j \neq i} |\langle i|\mu_m|j\rangle|^2 = \langle i|\mu_m^2|i\rangle$. Equation (66) can be further analysed depending on the relative values of L and \mathcal{Z} .

1. Thin layer ($\mathcal{Z}/L \gg 1$)

In this case the distance of the atom from the surface is much greater than the thickness of the layer of refractive index n_1 (but still small enough for the retardation to be neglected). Then, rescaling the integral in equation (66) with $k = x/L$ allows us to use Watson's lemma [22] to derive the following result

$$\Delta E^{\text{el}} \approx \Delta E_{n_s}^{\text{el}} - \frac{1}{64\pi\epsilon_0 \mathcal{Z}^3} \left(\langle \mu_{\parallel}^2 \rangle + 2\langle \mu_{\perp}^2 \rangle \right) \times \left[a_1 \frac{L}{\mathcal{Z}} + a_2 \frac{L^2}{\mathcal{Z}^2} + O\left(\frac{L^3}{\mathcal{Z}^3}\right) \right], \quad (67)$$

with the coefficients a_i given by

$$a_1 = \frac{3}{n_1^2} \frac{n_1^4 - n_s^4}{(n_s^2 + 1)^2},$$

$$a_2 = -\frac{6}{n_1^4} \frac{(n_1^4 - n_s^4)(n_s^2 + n_1^4)}{(n_s^2 + 1)^3},$$

where $\Delta E_{n_s}^{\text{el}}$ is the well-known electrostatic interaction energy between an atom and a dielectric half-space of refractive index n_s that can be obtained by the method of images

$$\Delta E_{n_s}^{\text{el}} = -\frac{1}{64\pi\epsilon_0 \mathcal{Z}^3} \frac{n_s^2 - 1}{n_s^2 + 1} \left(\langle \mu_{\parallel}^2 \rangle + 2\langle \mu_{\perp}^2 \rangle \right). \quad (68)$$

The corrections to this result are represented by the remaining elements of the asymptotic series. Note that if

$n_l > n_s$ then $a_1 > 0$ and, not surprisingly, the interaction, as compared to a half-space alone, is enhanced by the presence of the thin dielectric layer of higher refractive index n_l .

2. Thick layer ($Z/L \ll 1$)

In this case the thickness of the layer is much greater than the distance between the atom and the surface. The top layer now appears from the point of view of the atom almost as a half-space of refractive index n_l only that it is in fact of finite thickness. To analyse the result (66) in this limit we cast it in a somewhat different form. Note that, especially when kL is large but not only then,

$$\frac{n_l^2 - 1}{n_l^2 + 1} \frac{n_l^2 - n_s^2}{n_s^2 + n_l^2} e^{-2kL} < 1 \quad (69)$$

and the denominator of the integrand in Eq. (66) can be written as geometrical series. Since the series is absolutely convergent we can integrate it term by term and obtain the following representation of the electrostatic result

$$\begin{aligned} \Delta E^{\text{el}} &= \Delta E_{n_l}^{\text{el}} + \frac{1}{16\pi\epsilon_0} \left(\langle \mu_{\parallel}^2 \rangle + 2\langle \mu_{\perp}^2 \rangle \right) \frac{n_l^2}{n_l^4 - 1} \\ &\times \sum_{\nu=1}^{\infty} \left(\frac{n_l^2 - 1}{n_l^2 + 1} \frac{n_l^2 - n_s^2}{n_s^2 + n_l^2} \right)^{\nu} \frac{1}{(\mathcal{Z} + \nu L)^3} \quad (70) \end{aligned}$$

where $\Delta E_{n_l}^{\text{el}}$ is the electrostatic energy shift due to a single half-space of refractive index n_l , i.e. Eq. (68) with n_s replaced by n_l . The sum in Eq. (70) represents the correction to $\Delta E_{n_l}^{\text{el}}$ due to the finite thickness of the layer. For fixed \mathcal{Z} and L it can be easily computed numerically to any desired degree of accuracy. We note however, that to the leading order in \mathcal{Z}/L the interaction is weakened by the same amount independently of the

distance of the atom from the surface and therefore is not measurable. The next-to-leading order correction is the first to be distance-dependent and is proportional to \mathcal{Z}/L^4 , which can be easily seen by expanding the factor in series around $\mathcal{Z}/\nu L = 0$:

$$\frac{1}{(\mathcal{Z} + \nu L)^3} \approx \frac{1}{\nu^3 L^3} - \frac{3\mathcal{Z}}{\nu^4 L^4} + O\left(\frac{\mathcal{Z}^2}{L^5}\right). \quad (71)$$

B. Ground state atoms. Retarded limit, ($2\mathcal{Z}E_{ji} \gg 1$)

1. Thin layer ($\mathcal{Z}/L \gg 1$)

In this case we study the situation when the top layer is much thinner than the distance between the atom and the surface. To obtain the asymptotic series we use Watson's lemma in much the same way as in the electrostatic case [21]. Series expansion of the integrand in Eq. (58) about $x = 0$ decouples the integrals and the resulting integrals can be calculated analytically. Thus, to first approximation, for an atom located sufficiently far from the interface, the impact of the thin dielectric layer on the standard Casimir-Polder interaction can be described by

$$\begin{aligned} \Delta E^{\text{ret}} &= \Delta E_{n_s}^{\text{ret}} \\ &- \frac{1}{16\pi^2\epsilon_0\mathcal{Z}^4} \sum_{j \neq i} \left[\frac{a_{\parallel} |\mu_{\parallel}|^2 + 2a_{\perp} |\mu_{\perp}|^2}{E_{ji}} \right] \frac{L}{\mathcal{Z}} + O\left(\frac{L^2}{\mathcal{Z}^2}\right) \quad (72) \end{aligned}$$

where $\Delta E_{n_s}^{\text{ret}}$ is the retarded limit of energy shift caused by a single dielectric half-space of refractive index n_s , which was calculated in [9]. We give this result in Appendix C. The coefficients a_{\parallel} and a_{\perp} in (72) can be expressed in terms of elementary functions as

$$\begin{aligned} a_{\parallel} &= \frac{1}{n_l^2} \frac{n_l^2 - n_s^2}{(n_s^2 - 1)^2 (n_s^2 + 1)} \left[n_s^5 (6n_s - 3)(n_l^2 - 1) + 3n_s^2 (n_l^2 + 1) - n_l^2 (2n_s^4 + 3n_s^3 + 3n_s - 8) \right] \\ &- \frac{n_l^2 - n_s^2}{n_l^2 (n_s^2 - 1)^{5/2}} \ln \left(\sqrt{n_s^2 - 1} + n_s \right) \left[2n_s^2 n_l^2 (n_s^2 - 1)^2 - 2n_s^4 (n_s^2 - 1) + n_l^2 \right] \\ &- \frac{n_s^4}{2n_l^2} \frac{n_l^2 - n_s^2}{(n_s^2 - 1)^2 (n_s^2 + 1)^{3/2}} \ln \left(\frac{\sqrt{n_s^2 + 1} + 1}{\sqrt{n_s^2 + 1} - 1} \frac{\sqrt{n_s^2 + 1} - n_s}{\sqrt{n_s^2 + 1} + n_s} \right) \left[2n_s^4 (n_l^2 - 1) - 2n_s^2 - 3n_l^2 + 1 \right] \\ a_{\perp} &= \frac{1}{n_l^2} \frac{n_l^2 - n_s^2}{(n_s^2 - 1)^2 (n_s^2 + 1)} \left[n_s^4 (4n_s^2 - 3n_s - 3) - n_s^2 (12n_s^6 - 6n_s^5 + 2)(n_l^2 - 1) + n_l^2 (2n_s^6 + 7n_s^4 - 3n_s^3 + 2) \right] \\ &+ \frac{n_s^2}{n_l^2} \frac{n_l^2 - n_s^2}{(n_s^2 - 1)^{5/2}} \ln \left(\sqrt{n_s^2 - 1} + n_s \right) \left[n_l^2 (4n_s^6 - 6n_s^4 + 3n_s^2 - 1) - n_s^2 (2n_s^2 - 1)^2 \right] \\ &+ \frac{n_s^6}{2n_l^2} \frac{n_l^2 - n_s^2}{(n_s^2 - 1)^2 (n_s^2 + 1)^{3/2}} \ln \left(\frac{\sqrt{n_s^2 + 1} + 1}{\sqrt{n_s^2 + 1} - 1} \frac{\sqrt{n_s^2 + 1} - n_s}{\sqrt{n_s^2 + 1} + n_s} \right) \left[4n_s^4 (n_l^2 - 1) + 2n_s^2 (n_l^2 - 2) - 3n_l^2 + 1 \right] \end{aligned}$$

Both, a_{\parallel} and a_{\perp} , are positive for $n_1 > n_s$ so that, as one would expect, the interaction, as compared to a half-space alone, is enhanced by the thin dielectric layer of the higher refractive index n_1 . The above result simplifies significantly in the case when n_s approaches unity i.e. when the situation resembles that of an atom interacting with a dielectric slab of refractive index n_1 . The coefficients a_{\parallel} and a_{\perp} reduce then to those recently calculated in [1] and are given by

$$a_{\parallel} = \frac{(n_1^2 - 1)(9n_1^2 + 5)}{10n_1^2},$$

$$a_{\perp} = \frac{(n_1^2 - 1)(5n_1^2 + 4)}{10n_1^2}.$$

2. Thick layer ($Z/L \ll 1$)

Here we assume that the thickness of the top layer is much greater than the distance between the atom and the surface, but which is still large enough for retardation to occur. Note that the reflection coefficient \tilde{R}_{λ}^R (22) can be separated into L -dependent and L -independent parts in the following manner:

$$\tilde{R}_{\lambda}^R = r_{\lambda}^{vl} + \frac{[1 - (r_{\lambda}^{vl})^2] r_{\lambda}^{ls} e^{2ik_z L}}{1 + r_{\lambda}^{vl} r_{\lambda}^{ls} e^{2iLk_z L}}. \quad (73)$$

This way of writing the reflection coefficient splits the energy shift (58) into a shift due to the single interface of refractive index n_1 and corrections due to the finite thickness and the underlying material. It can be shown numerically, see Sec. V, that for large values of L the correction term is vanishingly small and can be safely discarded. Brute-force asymptotic analysis allows us to draw similar conclusions as in the electrostatic case, Section IV A 2. To leading order the interaction gets altered by the same amount regardless of the position of the atom with respect to the interface. The next-to-leading-order correction is proportional to Z/L^5 .

C. Excited atoms. Non-retarded limit, ($2Z|E_{ji}| \ll 1$)

The energy shift of an excited atom is given by equations (59) and (61). The "non-resonant" part, i.e. Eq. (59) has the same form as the energy shift of the ground state atom and has been analysed in the previous section. Therefore we now focus on the "resonant" part of the interaction that is given by equation (61). In order to conveniently obtain the non-retarded limit of (61) we will work with its slightly modified form given in equations (62) and (64).

We start by noting that close to the interface we expect asymptotic series to be in the inverse powers of Z . Equation (62), where the η integration runs over $\eta \in [0, 1]$,

contributes only positive powers of Z . This is most easily seen by expanding the exponential $\exp(2i|E_{ji}|Z\eta)$ about origin as we may do in the limit $2Z|E_{ji}| \rightarrow 0$. Therefore, to leading-order in the electrostatic limit, only (64) contributes. Further we analyse (64) by setting $\eta = \beta/(|E_{ji}|Z)$. Then, according to (65), in the limit $|E_{ji}|Z \rightarrow 0$ the wave vectors can effectively be approximated as

$$k_z \approx k_{z1} \approx k_{zs} \approx i \frac{\beta}{Z}. \quad (74)$$

Then the result for the energy shift, after substituting $\beta = kZ$, reduces to

$$\Delta E^{\text{res,el}} = -\frac{1}{8\pi\epsilon_0} \sum_{j < i} (|\mu_{\parallel}|^2 + 2|\mu_{\perp}|^2) \int_0^{\infty} dk k^2 e^{-2kZ}$$

$$\times \frac{\frac{n_1^2 - 1}{n_1^2 + 1} - \frac{n_1^2 - n_s^2}{n_s^2 + n_1^2} e^{-2kL}}{1 - \frac{n_1^2 - 1}{n_1^2 + 1} \frac{n_1^2 - n_s^2}{n_s^2 + n_1^2} e^{-2kL}}. \quad (75)$$

This result turns out to have the same dependence on Z and L as the Coulomb interaction of the ground state atom, cf. Eq. (66); therefore we shall not analyse Eq. (75) any further. Note however, that the dependence on the atomic states is different in equations (66) and (75). We would also like to point out that in the electrostatic limit, *to the order we are considering*, the quantity $\Delta E^{\text{res,el}}$ turns out to be real, which would imply that the corrections to the decay rates vanish. However, this conclusion is incorrect as it is known that the change of spontaneous emission in the non-retarded limit is in fact constant for a non-dispersive dielectric half-space [9]. However, any serious analysis of the changes of the decay rates induced by a surface needs to take into account the absorption of the material, which in the non-retarded limit plays a crucial role and cannot be neglected. Furthermore we note that we have started from Eq. (61), which, as explained before, contains poles on the real axis signalling the trapped modes. However, the denominator of (75) never vanishes which reflects the fact that in the electrostatic limit the trapped modes cease to exist and do not contribute towards the energy shifts, as first mentioned in [2].

D. Excited atoms. Retarded limit, ($2Z|E_{ji}| \gg 1$)

The leading-order behaviour of equation (61) in the retarded limit can be obtained by repeated integration by parts. Unlike in the electrostatic case now both equations, Eq. (62) and Eq. (64) contribute. We integrate them by parts and note that the non-oscillatory contributions that arise from the boundary terms evaluated at $\eta = 0$ cancel out. It turns out that the leading-order contributions to the energy shift are due to the perpendicular component of the atomic dipole moment. They

dominate the retarded interaction energy and behave as \mathcal{Z}^{-1} . The contributions due to the component of the atomic dipole moment that is perpendicular to the surface contribute only terms proportional to \mathcal{Z}^{-2} . We find that in the retarded limit the interaction energy up to the leading-order is given by

$$\begin{aligned} \Delta E_i^{\text{res,ret}} &= -\frac{1}{8\pi\epsilon_0\mathcal{Z}} \sum_{j<i} |E_{ji}|^2 |\mu_{\parallel}|^2 \\ &\times \frac{1}{1 + 2r_{\text{vl}}r_{\text{ls}} \cos(2|E_{ji}|\tau) + r_{\text{vl}}^2 r_{\text{ls}}^2} \\ &\times \{r_{\text{vl}}(1 + r_{\text{ls}}^2) \cos(2|E_{ji}|\mathcal{Z}) \\ &\quad + r_{\text{vl}}^2 r_{\text{ls}} \cos[2|E_{ji}|(\mathcal{Z} - \tau)] \\ &\quad + r_{\text{ls}} \cos[2|E_{ji}|(\mathcal{Z} + \tau)]\}, \quad (76) \end{aligned}$$

where we have defined the optical thickness of the layer as $\tau = n_1 L$ and

$$r_{\text{vl}} = \frac{1 - n_1}{1 + n_1}, \quad r_{\text{ls}} = \frac{n_1 - n_s}{n_1 + n_s}. \quad (77)$$

The final result agrees with that derived for a half-space in [9] if we take either $L \rightarrow 0$ or $n_1 \rightarrow n_s$, which is a consistency check of our calculation. However, the limit of perfect reflectivity of the top layer does not make sense and one has to start from equation (61) and rewrite the reflection coefficient in the form (73) in order to study this case.

Equation (76) is valid only approximately when the distance between the atom and the surface is much greater than the wavelength of the strongest atomic dipole transition, but it nevertheless allows us to draw important conclusions. We note that the interaction is resonant i.e. it is enhanced for certain values of LE_{ji} . The most convenient way to understand the essence of these resonance effects is to take the slab limit of equation (76) i.e. set $n_s = 1$. In this limit we have

$$\begin{aligned} \Delta E_i^{\text{res,ret}} &= -\frac{1}{8\pi\epsilon_0\mathcal{Z}} \sum_{j<i} |E_{ji}|^2 |\mu_{\parallel}|^2 \\ &\times \frac{1}{1 - 2r_{\text{vl}}^2 \cos(2|E_{ji}|\tau) + r_{\text{vl}}^4} \\ &\times \{r_{\text{vl}}(1 + r_{\text{vl}}^2) \cos(2|E_{ji}|\mathcal{Z}) \\ &\quad - r_{\text{vl}}^3 \cos[2|E_{ji}|(\mathcal{Z} - \tau)] \\ &\quad - r_{\text{vl}} \cos[2|E_{ji}|(\mathcal{Z} + \tau)]\}. \quad (78) \end{aligned}$$

It is easily seen that whenever $\cos(2|E_{ji}|\tau) = 1$ then $\Delta E_i^{\text{res,ret}} = 0$, i.e. the leading-order interaction vanishes. Conversely, the amplitude of oscillations in equation (78) is maximized when $\cos(2|E_{ji}|\tau) = -1$. Therefore we have a condition for resonance in terms of the wavelength of the strongest atomic dipole transition λ_{ji}

$$\tau = nL = \frac{\lambda_{ji}}{2} \left(\kappa + \frac{1}{2} \right), \quad \kappa = 0, 1, 2 \dots \quad (79)$$

Eq. (79) holds for $Z|E_{ji}| \gg 1$ but if the value of $Z|E_{ji}|$ approaches unity, the relation loses its validity, because

complications arise from the fact that when the atom is close to the surface the evanescent waves come into play whereas the condition (79) refers to the interaction of an atom with travelling modes only. In the non-retarded limit $\mathcal{Z}|E_{ji}| \ll 1$ the notion of resonance loses its meaning altogether, cf. Eq. (75). Exploring the extreme case in the retarded limit we note that at anti-resonance i.e. when

$$\tau = nL = \frac{\lambda_{ji}}{2} \kappa, \quad \kappa = 0, 1, 2 \dots \quad (80)$$

equation (76) becomes

$$\Delta E_i^{\text{res,ret}} = \frac{1}{8\pi\epsilon_0\mathcal{Z}} \frac{n_s - 1}{n_s + 1} \sum_{j<i} |E_{ji}|^2 |\mu_{\parallel}|^2 \cos(2|E_{ji}|\mathcal{Z}), \quad (81)$$

i.e. the atom does not feel the presence of the layer and the interaction assumes the form of that between an atom and a single half-space of refractive index n_s , cf. [9]. This means that in the retarded regime the leading-order interaction between an excited atom and a slab of thickness L vanishes whenever the optical thickness of the slab $\tau = n_1 L$ is equal to a half-integer multiple of the wavelength of the dominant atomic transition λ_{ji} (cf. also Fig. 11 later on). Conversely, at resonance the shift becomes

$$\Delta E_i^{\text{res,ret}} = \frac{1}{8\pi\epsilon_0\mathcal{Z}} \frac{n_1^2 - n_s}{n_1^2 + n_s} \sum_{j<i} |E_{ji}|^2 |\mu_{\parallel}|^2 \cos(2|E_{ji}|\mathcal{Z}), \quad (82)$$

so that the amplitude of oscillations exceeds the amplitude that would have been caused by a single half-space of refractive index n_1 . It also reaches the perfect reflector limit $n_1 \rightarrow \infty$ more rapidly. Finally, we shall also remark that the meaning of the conditions (79) and (80) is interchanged if the refractive index of the substrate n_s exceeds that of the layer n_1 i.e. when $n_s > n_1$.

V. NUMERICAL EXAMPLES

In this section we present a few numerical results designed to illustrate the influence of the dielectric layer on the Casimir-Polder interaction between an atom and a dielectric half-space. In practice, the sum over intermediate states j in Eq. (58) and in Eq. (61) is restricted to one or a few states to which there are strong dipole transitions. Hence, we assume a two-level system in which E_{ji} is a single number, namely the energy spacing of the levels with the strongest dipole transition. Additionally, we focus just on the contributions to the energy shift due to the component of the atomic dipole that is parallel to the interface of the dielectrics. The contributions due to the perpendicular components of the atomic dipole moment can be easily generated with from Eq. (58) using standard computer algebra packages like Mathematica or Maple. We start by simple checks on the asymptotic expansions derived in the previous section.

A. Ground-state atoms

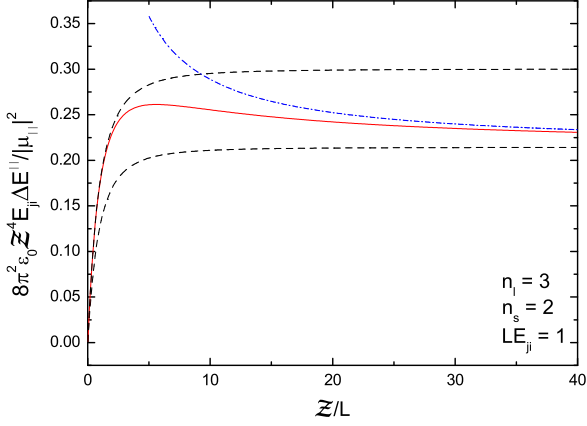


FIG. 5: Plot of the exact energy-level shift contributions ΔE^{\parallel} (solid), Eq. (58), multiplied by Z^4 . Dashed lines represent the energy shifts due to the single dielectric half-spaces of refractive indices n_1 (top) and n_s (bottom), whereas the dotted-dashed lines represents the asymptotic approximation (72).

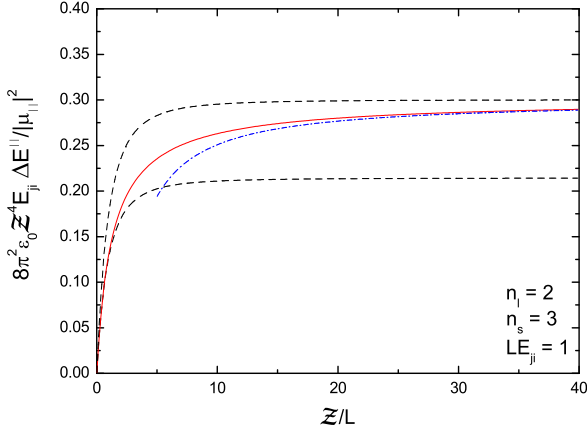


FIG. 6: Plot of the exact energy-level shift ΔE^{\parallel} (solid), Eq. (58), multiplied by Z^4 . Dashed lines represent the energy shifts due to the single dielectric half-spaces of refractive indices n_1 (bottom) and n_s (top), whereas the dotted-dashed lines represents the asymptotic approximation (72).

We choose to plot the energy-level shift ΔE multiplied by Z^4 so that the asymptotic behaviour of it as a function of distance is more apparent, because $Z^4 \Delta E$ for a dielectric half-space approaches constant [9]. Then, one can easily track the variation of the energy shift caused by the top layer as compared to the half-space shifts, Fig.

5 and Fig. 6. We remark that even though the derivation of the energy shift in this paper was based on the assumption $n_1 > n_s$, the results are also valid in the case when the top layer has a smaller reflectivity than the substrate. In such a case the result can be used e.g. to model a thin layer of oxide or any kind of dirt on the substrate which is often present under realistic conditions.

The asymptotic expansion (72) works well for large Z/L and not too high values of the refractive index n_1 . This is demonstrated in Fig. 7. The increase of the refractive index n_1 has an impact on the accuracy of the approximation which is valid provided

$$Z \gg \lambda_{ji} + \tau_1 \quad (83)$$

with λ_{ji} being the wavelength of the dominant atomic transition and $\tau_1 = n_1 L$ is the optical thickness of the top layer. In Fig. 8 we demonstrate the behaviour of

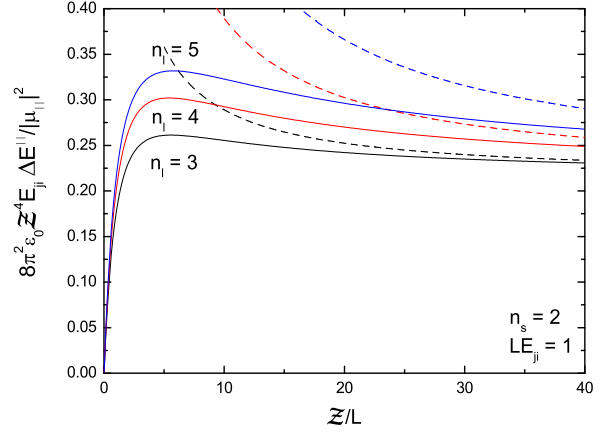


FIG. 7: Plot of the exact energy shift ΔE^{\parallel} , (solid, Eq. (58)), multiplied by Z^4 together with the asymptotic approximations (dashed, Eq. (72)).

the energy shift depending on the various values of the parameter E_{ji} measured in units of the layer's thickness. For small E_{ji} we clearly observe linear behaviour that corresponds to the Z^{-3} dependence of the shift in the electrostatic regime.

We also find it instructive to plot the energy-level shift as a function of the thickness of the top layer L for different values of the refractive index n_1 while keeping the distance of the atom from the surface fixed, Fig. 9 and Fig. 10.

B. Excited atoms

The energy shift of an excited atom splits into two distinct parts, cf. Eq. (59) and Eq. (61). The non-oscillatory part displays the same behaviour as the en-

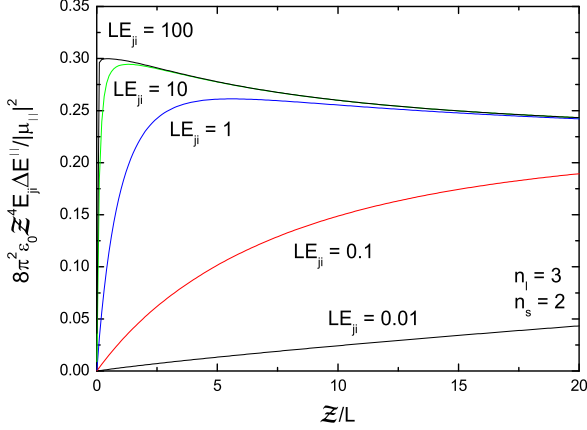


FIG. 8: Plot of the exact energy shift ΔE^{\parallel} (Eq. (58)) multiplied by Z^4 as a function of Z/L for various values of the retardation parameter $E_{ji}L$.

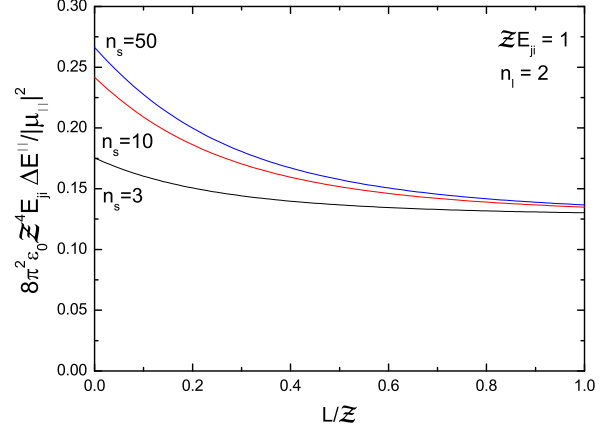


FIG. 10: Plot of the exact energy shift ΔE^{\parallel} (Eq. (58)) multiplied by Z^4 as a function of layer's thickness L measured in units of fixed atom-wall separation Z for various values of the substrate's refractive index $n_s > n_1$.

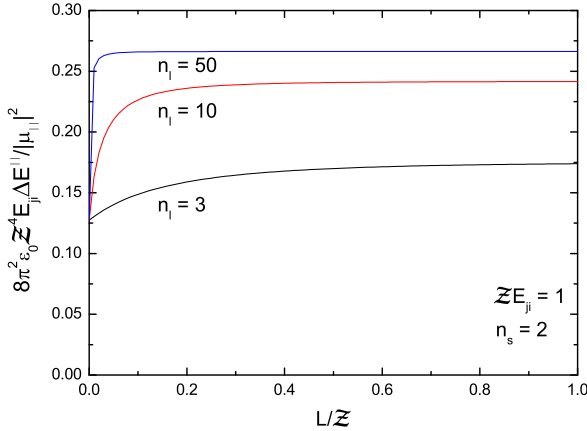


FIG. 9: Plot of the exact energy shift ΔE^{\parallel} (Eq. (58)) multiplied by Z^4 as a function of layer's thickness L measured in units of fixed atom-wall separation Z for various values of the layer's refractive index $n_1 > n_s$.

ergy shift of the ground-state atoms, which we have already analysed numerically in the previous section. Here we will focus on the oscillatory contributions to the level shifts that are given by Eq. (61). We choose to plot the dimensionless integrals contained in equations (62) and (64) as this is numerically more efficient than plotting the integral in Eq. (61). It should be borne in mind that the reflection coefficients contain the dispersion relation in denominators that now has solutions on the real axis. For the purpose of the present demonstration it is sufficient to simply displace the poles off the real axis by adding small imaginary part to the denominator of the re-

flexion coefficients, which amounts to taking the Cauchy principal-value during numerical integration. In Fig.

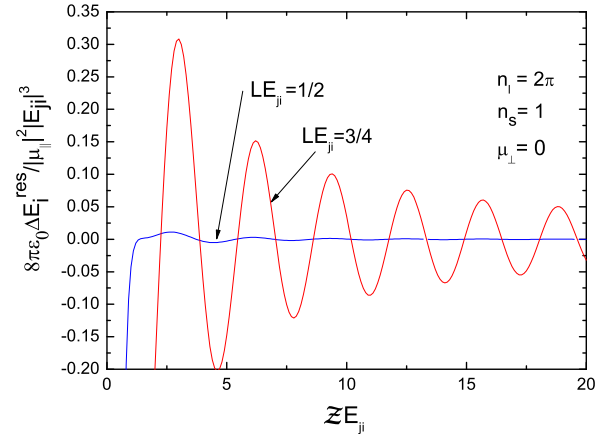


FIG. 11: Plot of the exact energy-level shift (61) (resonant part) in an excited atom due to the parallel component of the atomic dipole moment placed in front of a slab of thickness L and refractive index $n_1 = 2\pi$. The energy spacing of the dominant atomic transition is such that $LE_{ji} = 3/4$ i.e. it satisfies the resonance condition (80). As is seen, when $LE_{ji} = 1/2$, the energy shift in the retarded regime is strongly suppressed, cf. Eq. (76).

11 we demonstrate that indeed, if the anti-resonance condition (80) is satisfied, the interaction energy between the excited atom and the slab is strongly suppressed for $Z E_{ji} \gg 1$. In general, for the layered dielectric rather than the slab, the effect of resonance is shown in Fig. 12

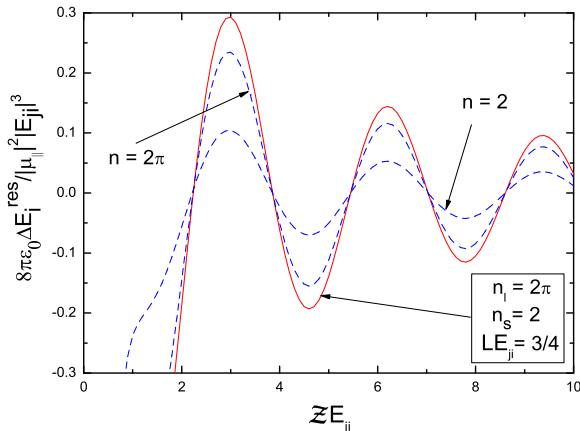


FIG. 12: Plot of the exact energy-level shift (61) (resonant part) in an excited atom due to the parallel component of the atomic dipole moment placed in front of the layered dielectric with parameters as shown on the graph (solid). The resonant condition (79) is satisfied so that the interaction is enhanced. The amplitude of oscillations exceeds the one that would have been caused by an unlayered half-space of the refractive index $n = 2\pi$, cf. Eq. (81). Compare also Fig. 5. The dashed lines represent the interaction between an atom and single half-space of refractive index n as indicated.

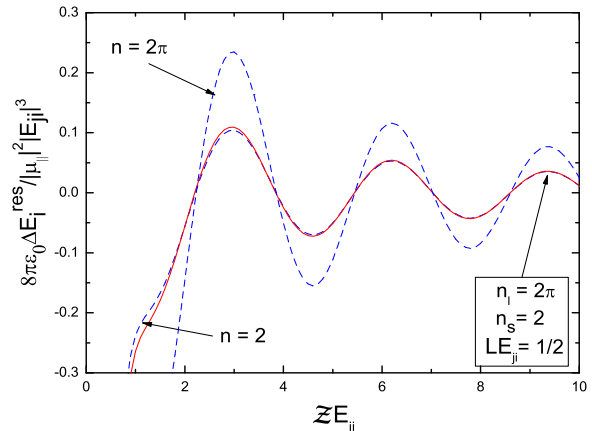


FIG. 13: Plot of the exact energy-level shift (61) (resonant part) in an excited atom due to the parallel component of the atomic dipole moment placed in front of the layered dielectric with parameters as shown on the graph (solid). The anti-resonant condition (80) is satisfied so that the presence of the layer is almost unnoticeable, cf. Eq. (81). The dashed lines represent the interaction between an atom and single half-space of refractive index n as indicated.

VI. SUMMARY

and Fig. 13. Note that the energy-level shift in an excited atom due to the layered dielectric can be significantly enhanced. Unlike in the case of the ground state atom where the energy shift caused by the layered structure of refractive indices n_1 and n_s is bounded by the single half-space shifts (compare Fig. 5), the excited atom can experience shifts greater than those caused by the unlayered half-space of the refractive index $n = \max(n_1, n_s)$, Fig. 12, which is due to resonance effects. Conversely, it is also possible that the interaction with the layer will be unnoticeable if the anti-resonance condition (80) is satisfied, Fig. 13. Next, in Fig. 14, we show that the approximation of Eq. (61) derived in (76) turns out to be quite accurate and can be safely used to quickly estimate the energy shift in an excited atom caused by the layered dielectric, provided the condition $ZE_{ji} \gg 1$ is satisfied. It is also interesting to plot the resonant part of the energy shift as a function of LE_{ji} while keeping ZE_{ji} fixed. This is done in Fig. 15. It is seen that the energy shift indeed experiences the oscillatory resonant behaviour. The subsequent minima and maxima are less and less pronounced as the value of LE_{ji} increases. This is because as we increase LE_{ji} the resonances and anti-resonances move closer and closer together so that their effects cancel out. It is interesting to note that this behaviour could not have been inferred from equation (76), which indicates that the approximation (76) can be useful only for $LE_{ji} \ll 1$, which can also be easily verified numerically.

Using perturbation theory we have calculated the energy-level shift in a neutral atom placed in front of a layered dielectric half-space, as shown in Fig. 1. The major difficulty in working out the energy shift is the sum over all modes that appears in this type of calculation, Eq. (50), especially when the spectrum of the modes consists of the continuous and discrete parts, Sec. II A and II B. This obstacle can be circumvented by using complex-variable techniques to express the sum over all modes as a single contour integral in the complex k_z -plane, Eq. (54) and Fig. 4. Then, the energy shift (58) is easily analyzed asymptotically as well as numerically. For a ground-state atom, regardless of whether in retarded or non-retarded regimes, we find that the leading-order correction to the interaction of an atom with an unlayered interface is proportional to L/Z . The asymptotic series are given by (67) and (72) and provide reasonable estimate of the influence of the single dielectric layer on the standard half-space result, Fig. 7. In the opposite case of a very thick layer i.e. $Z/L \ll 1$ we find that the result is well approximated by a dielectric half-space [9]. For excited atoms we find that the interaction between an atom and the layered dielectric (61) is subject to resonances that occur between the wavelength of the dominant atomic transition λ_{ji} and the thickness of the layer L , Sec. IVD. In particular, the interaction between an atom and the slab can be strongly suppressed in the retarded regime, cf. Fig. 11, whenever the optical

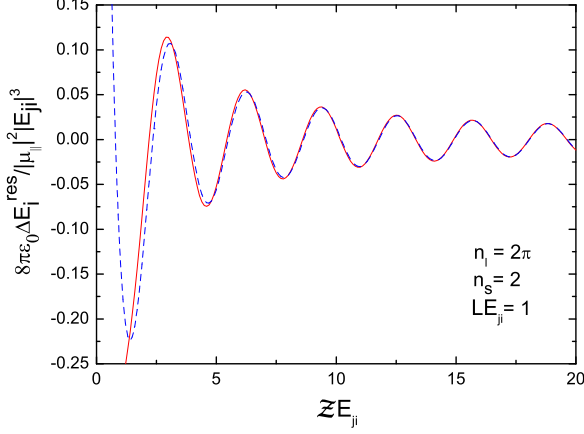


FIG. 14: Plot of the exact energy-level shift (61) (resonant part) in an excited atom due to the parallel component of the atomic dipole moment placed in front of the layered dielectric with parameters as shown on the graph (solid). The dashed line represents the approximation in the retarded regime, Eq. (76).

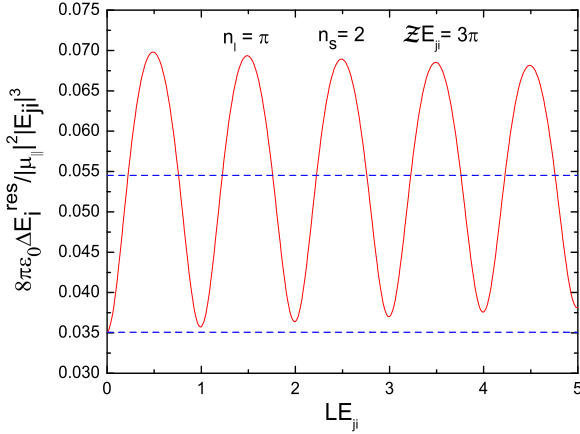


FIG. 15: Plot of the exact energy-level shift (61) (resonant part) in an excited atom due to the parallel component of the atomic dipole moment placed in front of the layered dielectric with parameters as shown on the graph (solid). The dashed lines represent energy shifts caused by the single half-spaces of refractive index $n_1 = 2\pi$ (top) and $n_s = 2$ (bottom).

thickness of the slab τ is equal to the half-integer multiple of the wavelength of the dominant atomic transition λ_{ji} . The existence of resonance effects suggests a physical picture of the excited atom as a radiating dipole. The resonance and anti-resonance correspond to constructive and destructive interference. We have also provided reasonable approximations in the non-retarded (75) and re-

tarded (76) regimes that can be used to quickly estimate the magnitude of the resonant interaction between an atom and a layered dielectric.

Appendix A: Fresnel coefficients for layered dielectric

Here we list the reflection and transmission coefficients appearing in the normal-modes of the system as discussed in the section II A. For the left-incident modes we find

$$\begin{aligned} R_\lambda^L &= \frac{r_\lambda^{sl} + r_\lambda^{lv} e^{2ik_{z1}L}}{1 + r_\lambda^{sl} r_\lambda^{lv} e^{2ik_{z1}L}} e^{-ik_{zs}L} \\ I_\lambda^L &= \frac{t_\lambda^{sl} e^{i(k_{z1} - k_{zs})L/2}}{1 + r_\lambda^{sl} r_\lambda^{lv} e^{2ik_{z1}L}} \\ J_\lambda^L &= \frac{t_\lambda^{sl} r_\lambda^{lv} e^{(3ik_{z1} - ik_{zs})L/2}}{1 + r_\lambda^{sl} r_\lambda^{lv} e^{2ik_{z1}L}} \\ T_\lambda^L &= \frac{t_\lambda^{sl} t_\lambda^{lv} e^{(2ik_{z1} - ik_{zs} - ik_z)L/2}}{1 + r_\lambda^{sl} r_\lambda^{lv} e^{2ik_{z1}L}}, \end{aligned}$$

and for the right-incident modes we get

$$\begin{aligned} R_\lambda^R &= \frac{r_\lambda^{vl} + r_\lambda^{ls} e^{2ik_{z1}L}}{1 + r_\lambda^{vl} r_\lambda^{ls} e^{2ik_{z1}L}} e^{-ik_zL} \\ I_\lambda^R &= \frac{t_\lambda^{vl} e^{i(k_{z1} - k_z)L/2}}{1 + r_\lambda^{vl} r_\lambda^{ls} e^{2ik_{z1}L}} \\ J_\lambda^R &= \frac{t_\lambda^{vl} r_\lambda^{ls} e^{(3ik_{z1} - ik_z)L/2}}{1 + r_\lambda^{vl} r_\lambda^{ls} e^{2ik_{z1}L}} \\ T_\lambda^R &= \frac{t_\lambda^{vl} t_\lambda^{ls} e^{(2ik_{z1} - ik_{zs} - ik_z)L/2}}{1 + r_\lambda^{vl} r_\lambda^{ls} e^{2ik_{z1}L}}. \end{aligned}$$

The Fresnel reflection coefficients r_λ^{ab} for a single interface are given by (11).

Appendix B: Electrostatic calculation of the energy-level shift in a ground-state atom in a layered geometry

To provide an additional check on the consistency of our calculations we would like to derive equation (66) by means of electrostatics. We start from the general formula derived in [20] that expresses the electrostatic interaction energy of a electric dipole in the presence of a dielectric in terms of Green's function of the Laplace equation

$$\Delta E = \frac{1}{2} \sum_i \langle \mu_i^2 \rangle \nabla_i \nabla'_i G_H(\mathbf{r}, \mathbf{r}') \Big|_{\mathbf{r}=\mathbf{r}_0, \mathbf{r}'=\mathbf{r}_0}. \quad (\text{B1})$$

Here the sum runs over three components of the dipole moment and the subscript H means that only the homogeneous correction to the free-space Green's function that is caused by the presence of the boundary enters the

formula. This ensures that the self-energy of the dipole is omitted and guarantees the convergence of the final result. The harmonic function $G_H(\mathbf{r}, \mathbf{r}')$ is a solution of the Laplace equation that vanishes for $|z| \rightarrow \infty$. Therefore it can be written in the form:

$$G_H(\mathbf{r}, \mathbf{r}') = -\frac{1}{4\pi\epsilon_0} \int_0^\infty d_2 \mathbf{k}_\parallel e^{i\mathbf{k}_\parallel \cdot \mathbf{r}_\parallel} \times \begin{cases} C_1(\mathbf{k}_\parallel, \mathbf{r}') e^{k_z z} & z < L/2 \\ C_2(\mathbf{k}_\parallel, \mathbf{r}') e^{k_z z} + C_3(\mathbf{k}_\parallel, \mathbf{r}') e^{-k_z z} & |z| < L/2 \\ C_4(\mathbf{k}_\parallel, \mathbf{r}') e^{-k_z z} & z > L/2 \end{cases}, \quad (\text{B2})$$

with $k_z = \sqrt{k_x^2 + k_y^2}$. The C coefficients are easily worked out by applying the continuity conditions, which result from Maxwell's equations, across the interfaces and one finds that

$$G_H(\mathbf{r}, \mathbf{r}') = -\frac{1}{4\pi\epsilon_0} \int_0^\infty dk J_0(k\rho) e^{-k(z+z')} \times \frac{\frac{n_1^2 - 1}{n_1^2 + 1} - \frac{n_1^2 - n_s^2}{n_s^2 + n_1^2} e^{-2kL}}{1 - \frac{n_1^2 - 1}{n_1^2 + 1} \frac{n_1^2 - n_s^2}{n_s^2 + n_1^2} e^{-2kL}} \quad (\text{B3})$$

with $\rho = \sqrt{(x-x')^2 + (y-y')^2}$. Application of the formula (B1) is straightforward and we easily derive that the electrostatic interaction energy of a dipole in a vicinity of the layered dielectric is indeed equal to (66).

Appendix C: Retarded limit of the interaction energy between an atom and a dielectric half-space

The interaction between an atom and a non-dispersive dielectric half-space has been considered in detail in [9].

It has been shown there that, to leading-order, the energy shift in the retarded limit can be expressed as

$$\Delta E_{n_s}^{\text{ret}} = -\frac{3}{64\pi^2\epsilon_0 Z^4} \sum_{j \neq i} \left(\frac{c_{\parallel} |\mu_{\parallel}|^2 + c_{\perp} |\mu_{\perp}|^2}{E_{ji}} \right), \quad (\text{C1})$$

with the coefficients $c_{\parallel, \perp}$ given by

$$\begin{aligned} c_{\parallel} &= -\frac{1}{n_s^2 - 1} \left(\frac{2}{3} n_s^2 + n_s - \frac{8}{3} \right) \\ &+ \frac{2n_s^4}{(n_s^2 - 1)\sqrt{n_s^2 + 1}} \ln \left(\frac{\sqrt{n_s^2 + 1} + 1}{n_s [\sqrt{n_s^2 + 1} + n_s]} \right) \\ &+ \frac{2n_s^4 - 2n_s^2 - 1}{(n_s^2 - 1)^{3/2}} \ln \left(\sqrt{n_s^2 + 1} + n_s \right), \\ c_{\perp} &= \frac{1}{n_s^2 - 1} \left(4n_s^4 - 2n_s^3 - \frac{4}{3}n_s^2 + \frac{4}{3} \right) \\ &- \frac{4n_s^6}{(n_s^2 - 1)\sqrt{n_s^2 + 1}} \ln \left(\frac{\sqrt{n_s^2 + 1} + 1}{n_s [\sqrt{n_s^2 + 1} + n_s]} \right) \\ &- \frac{2n_s^2(2n_s^4 - 2n_s^2 + 1)}{(n_s^2 - 1)^{3/2}} \ln \left(\sqrt{n_s^2 - 1} + n_s \right). \end{aligned}$$

-
- [1] C. Eberlein, A. Contreras Reyes, Phys. Rev. A **80**, 032901(2009).
[2] J. M. Wylie, and J.E. Sipe, Phys. Rev. A **32**, 2030(1985).
[3] S.Y. Buhmann, D.-G. Welsh, Progress in Quantum Electronics, **31**, 51 (2007)
[4] A.D. McLachlan, Proc. R. Soc. London, Series A **271**, 387 (1963)
[5] S.Y. Buhmann, L. Knoll, D.-G. Welsh, H. Dung, Phys. Rev. A **70**, 052117(2004).
[6] J. M. Wylie, and J.E. Sipe, Phys. Rev. A **30**, 1185(1984).
[7] C.K. Carniglia and L. Mandel, Phys. Rev. D **3**, 280(1971).
[8] H. Koshravi and R. Loudon, Proc. R. Soc. London, Series A **433**, 337 (1991); *ibid.* **436**, 373, (1992).
[9] S. Wu and C. Eberlein, Proc. R. Soc. London, Series A **455**, 2487 (1998)
[10] M. Bordag, Phys. Rev. D **70**, 085010(2004); *ibid.* **76**, 065011, (2007).
[11] E. Yablonoitch, T.J. Gmitter and R. Bhat, Phys. Rev. Lett. **61**, 2546 (1988).
[12] R. Glauber, M. Levenstein Phys. Rev. A **43**, 467(1991).
[13] J.D. Jackson, *Classical Electrodynamics* (Wiley, New York, 1962).
[14] R. Zietal, DPhil thesis (University of Sussex, Brighton, 2010), (unpublished).
[15] *Handbook of Mathematical Functions*, edited by M. Abramowitz and I. Stegun (US GPO, Washington, DC, 1964).
[16] H.P. Urbach and G.L.J.A. Rikken, Phys. Rev. A **57**, 3913(1998).
[17] C. Eberlein, A. Contreras Reyes, Phys. Rev. A **79**, 043834(2009).
[18] I. Bialynicki-Birula and J.B. Brojan, Phys. Rev. D **5** 485 (1972)
[19] C. Eberlein and D. Robashik, Phys. Rev. D **73**, 025009(2006).
[20] C. Eberlein and R. Zietal, Phys. Rev. A **75**, 032516 (2007).
[21] C.M. Bender, S. A. Orszag, *Advanced Mathematical Methods for Scientists and Engineers*, (Springer Sci-

ence+Business Media, Inc. 1999).

[22] The essential idea is to spot that, since the integrand is strongly damped by the exponential, most of the contributions to the integral will come from small values of k .

Thus, it is permissible to Taylor-expand the remaining part of the integrand about $k = 0$. For a more rigorous treatment see [21].

